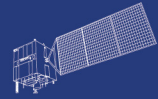


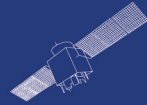
HY



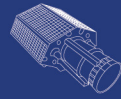
HJ-1AB



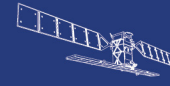
CBERS



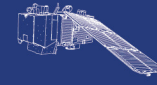
Gaofen



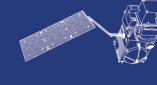
Beijing-2



Sentinel-1



Sentinel-2



Sentinel-3



Sentinel-5p



Aeolus

2023 DRAGON 5 SYMPOSIUM

3rd YEAR RESULTS REPORTING

11-15 SEPTEMBER 2023

PROJECT ID. 59333

**EO-AI4Urban: Earth Observation Big Data & Deep Learning
for Sustainable And Resilient Cities**

<WEDNESDAY, SEPTEMBER 13, 2023>

ID. 59333

PROJECT TITLE: EO-AI₄URBAN - EARTH OBSERVATION BIG DATA AND DEEP LEARNING FOR SUSTAINABLE AND RESILIENT CITIES

PRINCIPAL INVESTIGATORS: YIFANG BAN & YUNMING YE

CO-AUTHORS: YIFANG BAN, YUNMING YE, PAOLO GAMBA, PEIJUN DU, KUN TAN, LINLIN LU

PRESENTED BY: YIFANG BAN, SEBASTIAN HAFNER, KUN TAN, LINLIN LU

- Inform on the project's objectives
- Detail the Copernicus Sentinels, ESA, Chinese and ESA Third Party Mission data utilised after 3 years (complete slide 4)
- Detail the in-situ data measurements and requirements
- Provide details on field data collection campaigns and periods in P.R. China or other study areas
- Inform on the results after 3 years of activity
- Inform on the project's schedule, planning & contribution of the partners for the following year
- Report on the level and training of young scientists on the project achievements, including plans for academic exchanges
- Report on the peer reviewed publications (nr. of papers, journal name and publication title) after 3 years of activity

- The overall objective is to develop innovative, robust and globally applicable methods, based on EO big data and deep learning, for urban mapping and urbanization monitoring to support sustainable and resilient urban development.



- Evaluate Sentinel-1 SAR and Sentinel-2 MSI time series, Chinese EO data and ESA TPM data for improved urban mapping and change detection in both 2D and 3D;
- Develop novel and efficient methods for **urban mapping** with Sentinel-1 SAR and Sentinel-2 MSI time series and deep learning;
- Develop innovative and robust methods for **continuous urban change detection** using Sentinel-1 SAR and Sentinel-2 MSI time series and deep learning;
- Evaluate SAR-based method for **3D urban change estimation**;
- Assess the **environmental impact of urbanization** at local and landscape scales, and to evaluate the potential of the urban extent and change information derived from the Sentinel big data for monitoring the indicators of the UN 2030 SDG11, Sustainable Cities and Communities.

European PI	European YS	Affiliation
Yifang Ban	PhD student: Sebastian Hafner	KTH, Stockholm, Sweden

Chinese PI	Chinese YS	Affiliation
Yunming Ye	PhD student: Yuxi Sun	Harbin Institute of Technology, Shengzhen

European Co-PIs	European YS	Affiliation
Paolo Gamba	PhD student: Luigi Russo	University of Pavia, Italy

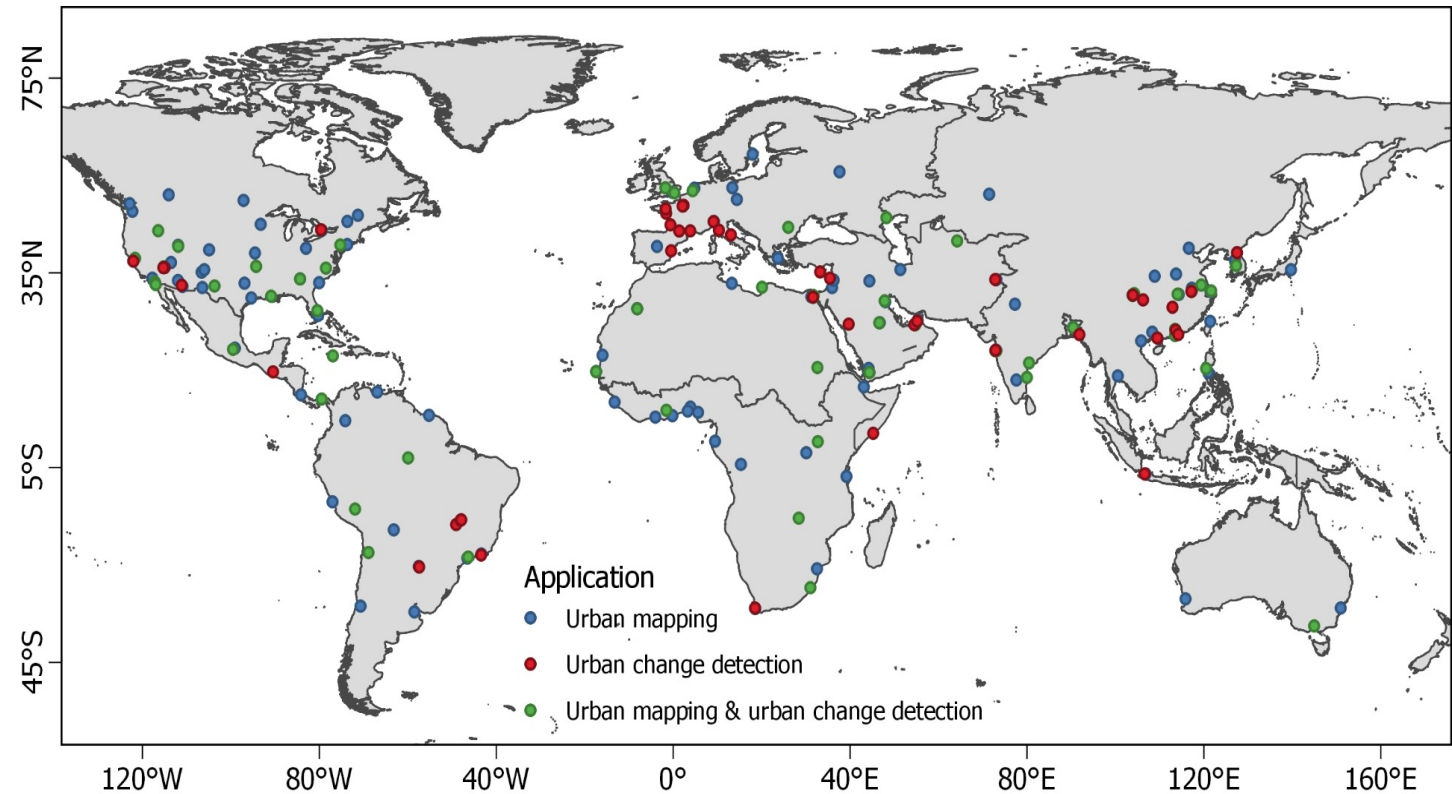
Chinese Co-PIs	Chinese YS	Affiliation
Peijun Du	PhD student: Xiaoquan Pan	Nanjing University
Kun Tan	PhD student: Renjie Ji	East China Normal University, Shanghai
Linlin Lu	PhD student: Liying Han	Aerospace Information Research Institute, CAS

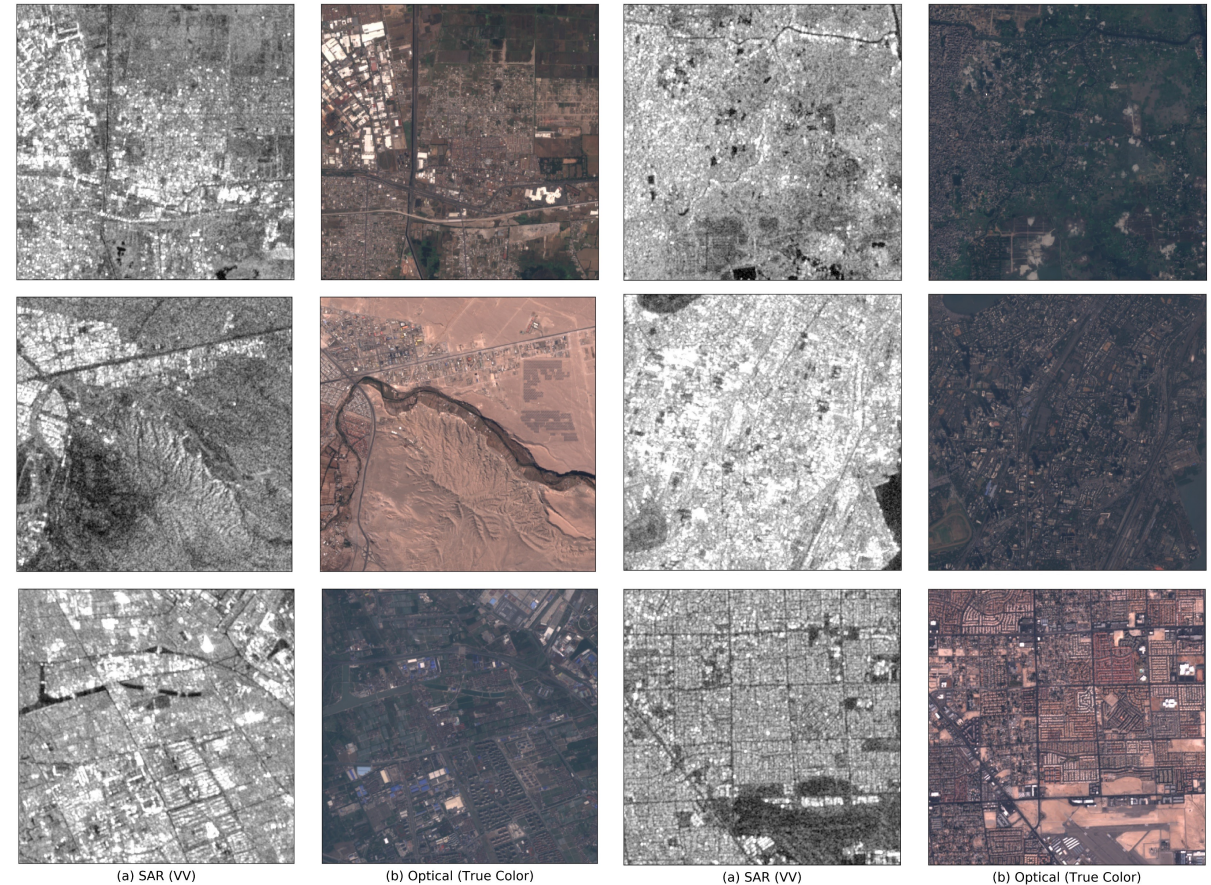
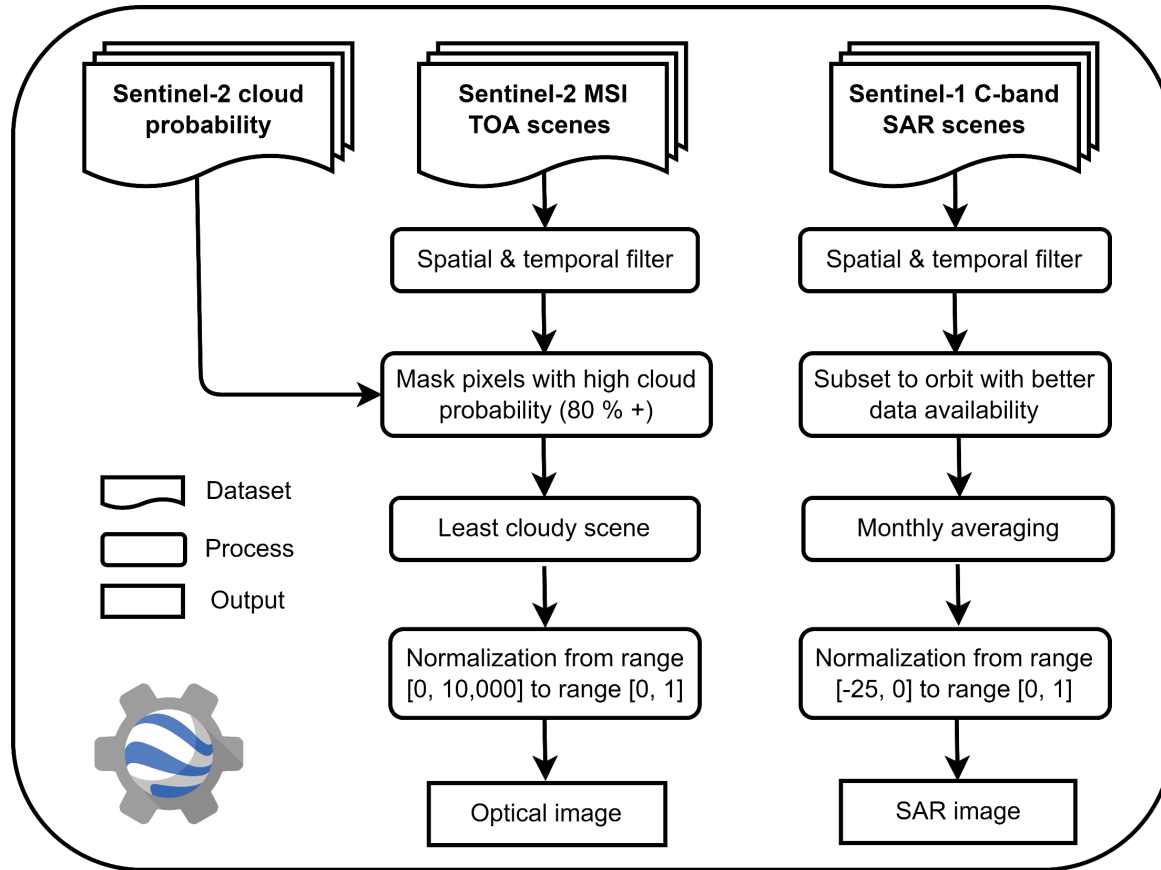
Data access (list all missions and issues if any). NB. in the tables please insert cumulative figures (since July 2020) for no. of scenes of high bit rate data (e.g. S1 100 scenes). If data delivery is low bit rate by ftp, insert “ftp”

ESA /Copernicus Missions	No. Scenes	ESA Third Party Missions	No. Scenes	Chinese EO data	No. Scenes
1. Sentinel-1	2200	1. TerraSAR-X	30	1. GF-1	30
2. Sentinel-2	600	2. Cosmo-SkyMed	50	2. GF-2	30
3.		3. RADARSAT-2, RCM	50	3. GF-3	50
4.		4. Landsat	50	4. ZY-3	50
5.		5.		5.	
6.		6.		6.	
Total:	2800	Total:	180	Total:	160
Issues:		Issues:		Issues:	

Locations of study sites grouped by application

- Over 200 study sites
- Covering six continents
- Leverage existing datasets for labels
- Add preprocessed Sentinel-1/2 data



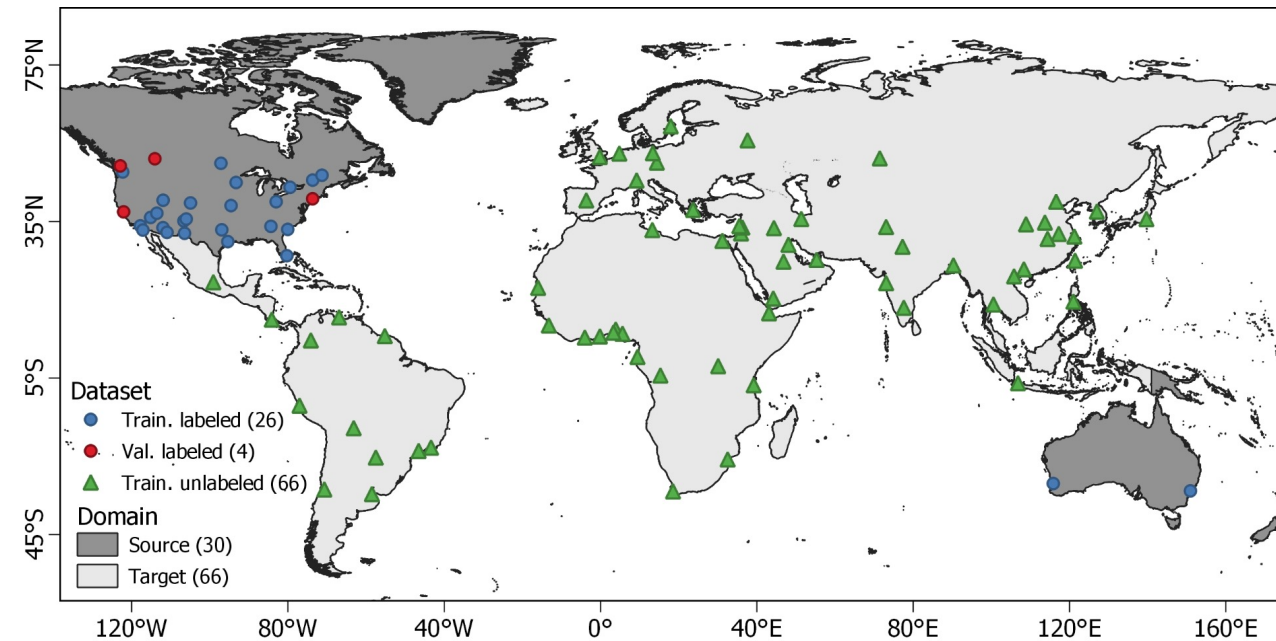


- Microsoft Building Footprints as labels



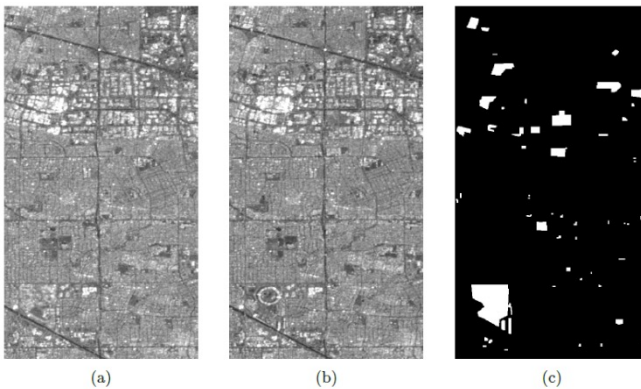
- Introduce a domain gap
- Produced Sentinel-1/2 data and corresponding labels

Locations of the training and validation sites

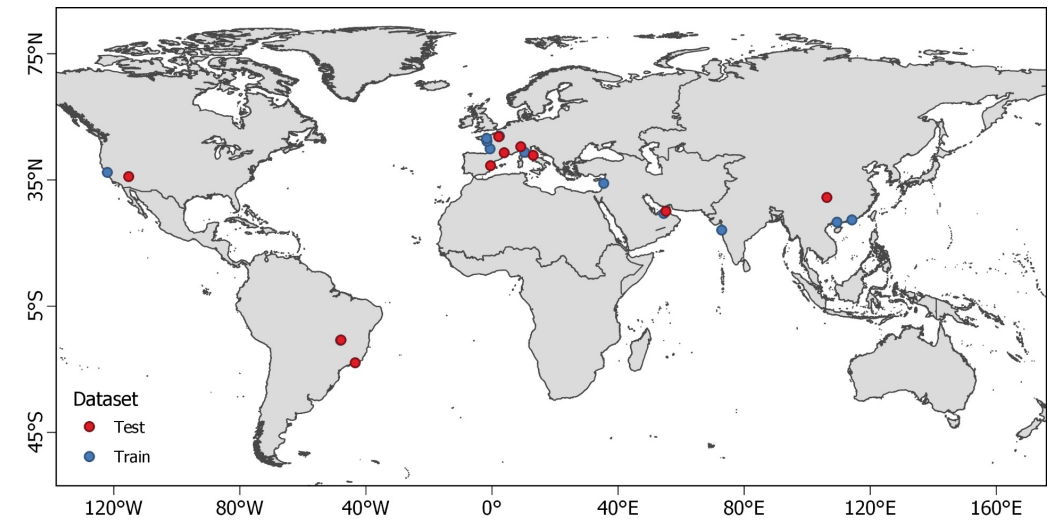


Microsoft. Microsoft releases 125 million building footprints in the US as open data, 2018.
 URL <https://blogs.bing.com/maps/2018-06/microsoft-releases-125-million-building-footprints-in-the-us-as-open-data>.

- Onera Satellite Change Detection (OSCD) dataset
- 24 Sentinel-2 image pairs
- Corresponding urban change labels
- Produced Sentinel-1 data for each site (incl. different orbits)



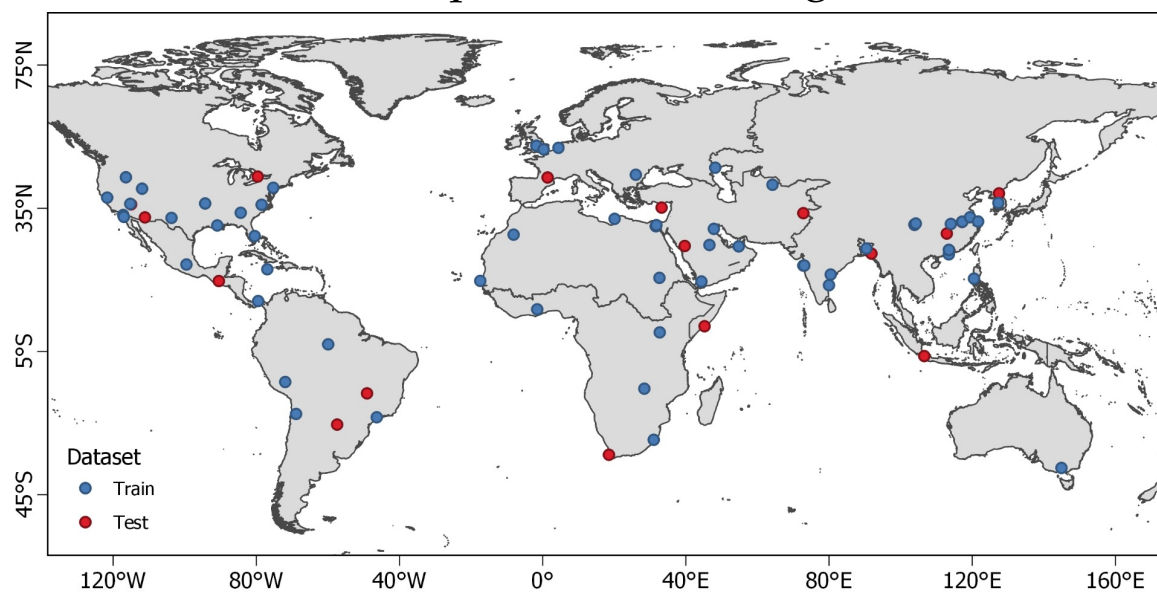
Locations of the training and test sites



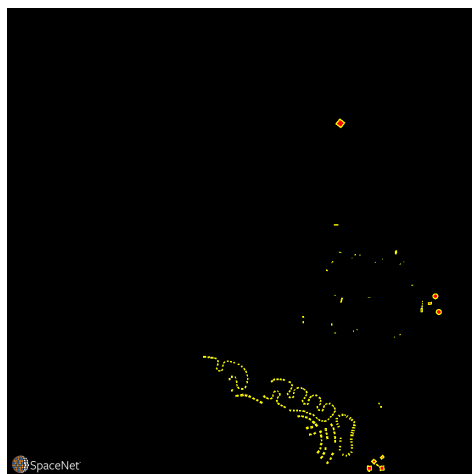
Daudt, R.C., Le Saux, B., Boulch, A. and Gousseau, Y., 2018, July. Urban change detection for multispectral earth observation using convolutional neural networks. In *IGARSS 2018-2018 IEEE International Geoscience and Remote Sensing Symposium* (pp. 2115-2118).

- Time series of monthly Planet images
- Covering ~ 100 unique sites
- Approximately 24 images per site
- Over 10 million individual annotated building footprints

Locations of the SpaceNet7 training and test sites

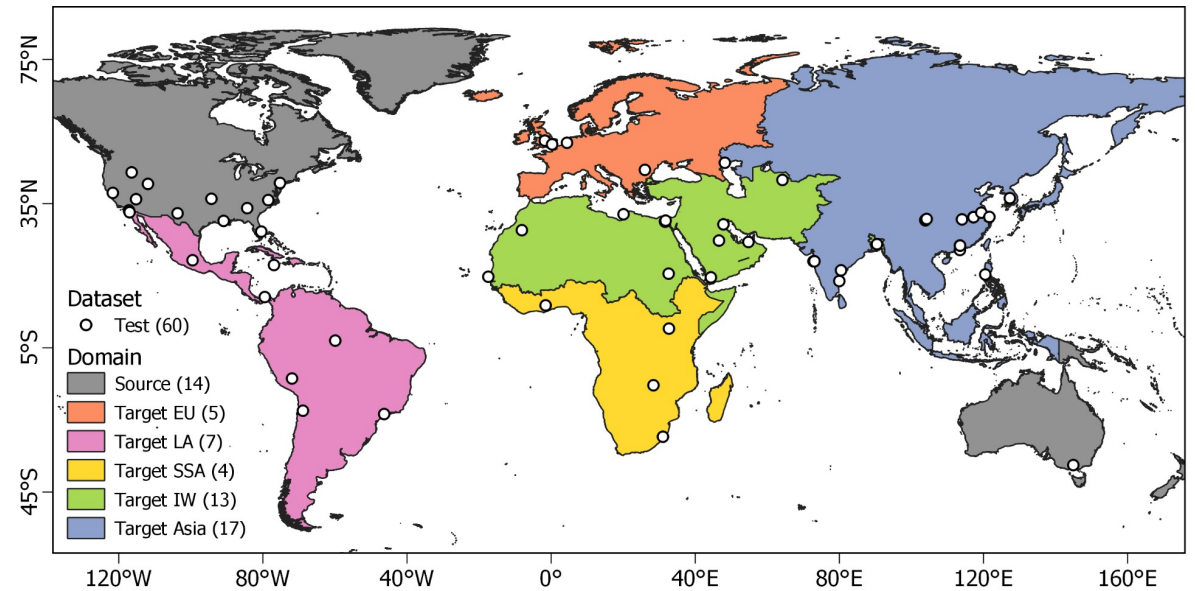


Van Etten, A., Hogan, D., Manso, J.M., Shermeyer, J., Weir, N. and Lewis, R., 2021. The multi-temporal urban development spacenet dataset. In *Proceedings of the IEEE/CVF Conference on Computer Vision and Pattern Recognition* (pp. 6398-6407).



- 60 SpaceNet7 training sites adopted as test sites
- Selected a single timestamp from each time series
- Produced Sentinel-1/2 data and corresponding label
- Introduced a domain gap
- Grouped target domain sites by cultural/geographic regions

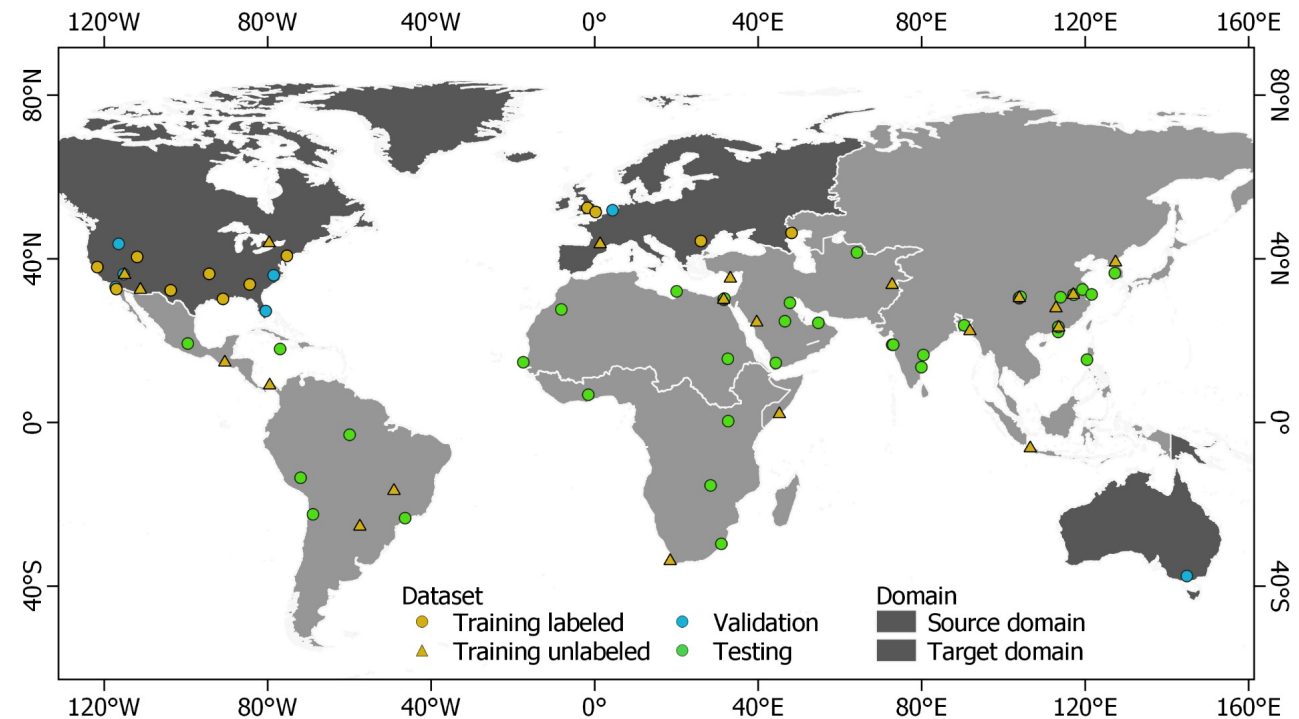
Locations of the test sites adopted from the SpaceNet7 training sites

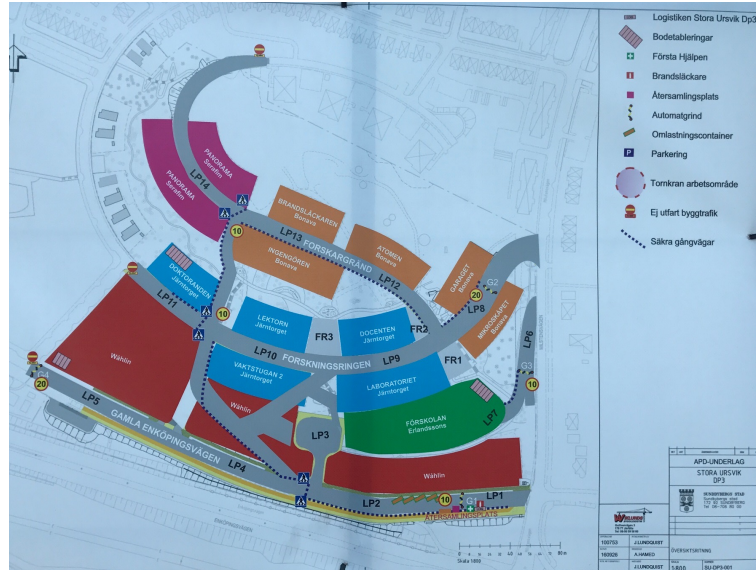


EU: Europe; LA: Latin America; SSA: Sub-Saharan Africa; IW: Islamic World.

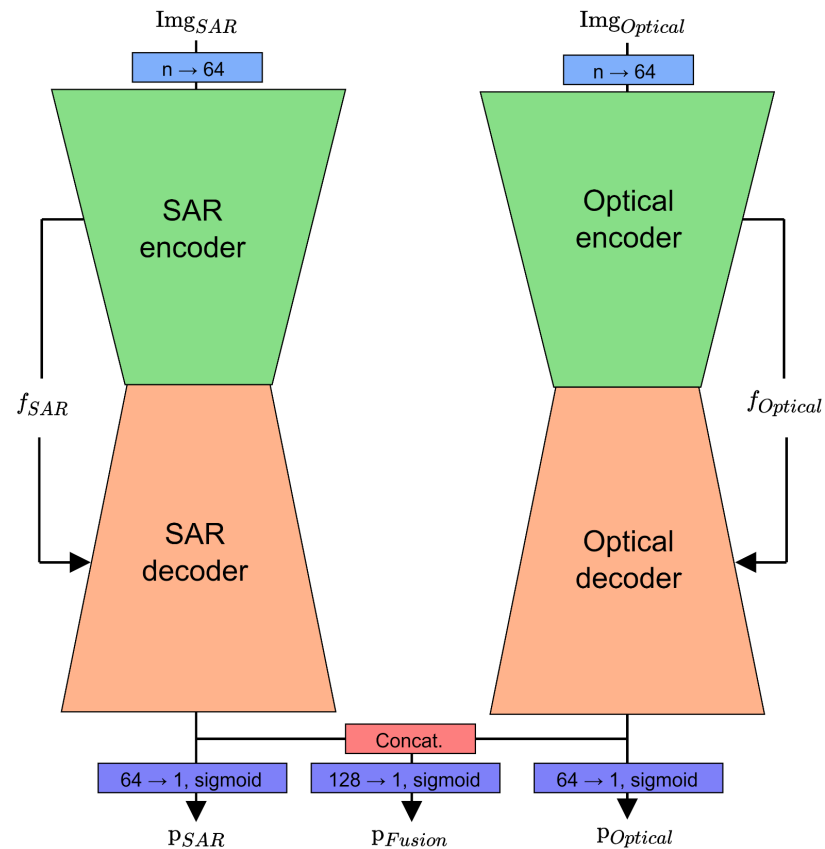
- Training, validation and testing with SpaceNet7 sites
- Introduced a domain gap
- Used SpaceNet7 training sites for labeled training, validation and testing
- Used SpaceNet7 test sites for unlabeled training
- Produced Sentinel-1/2 data and corresponding label

Locations of the training, validation and test sites

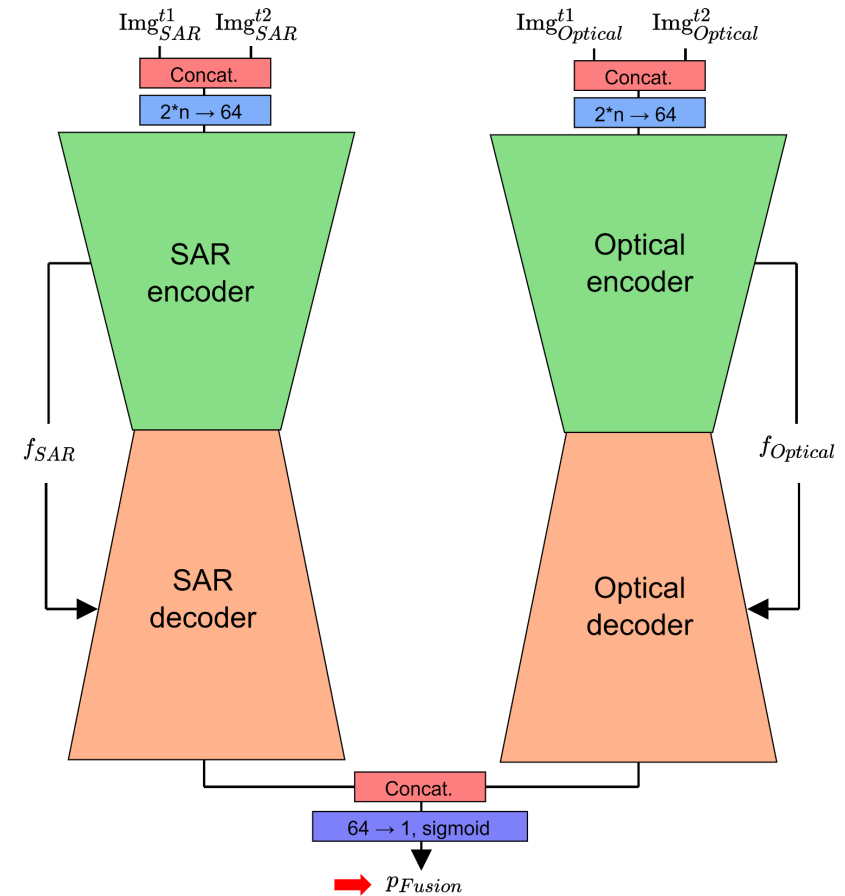




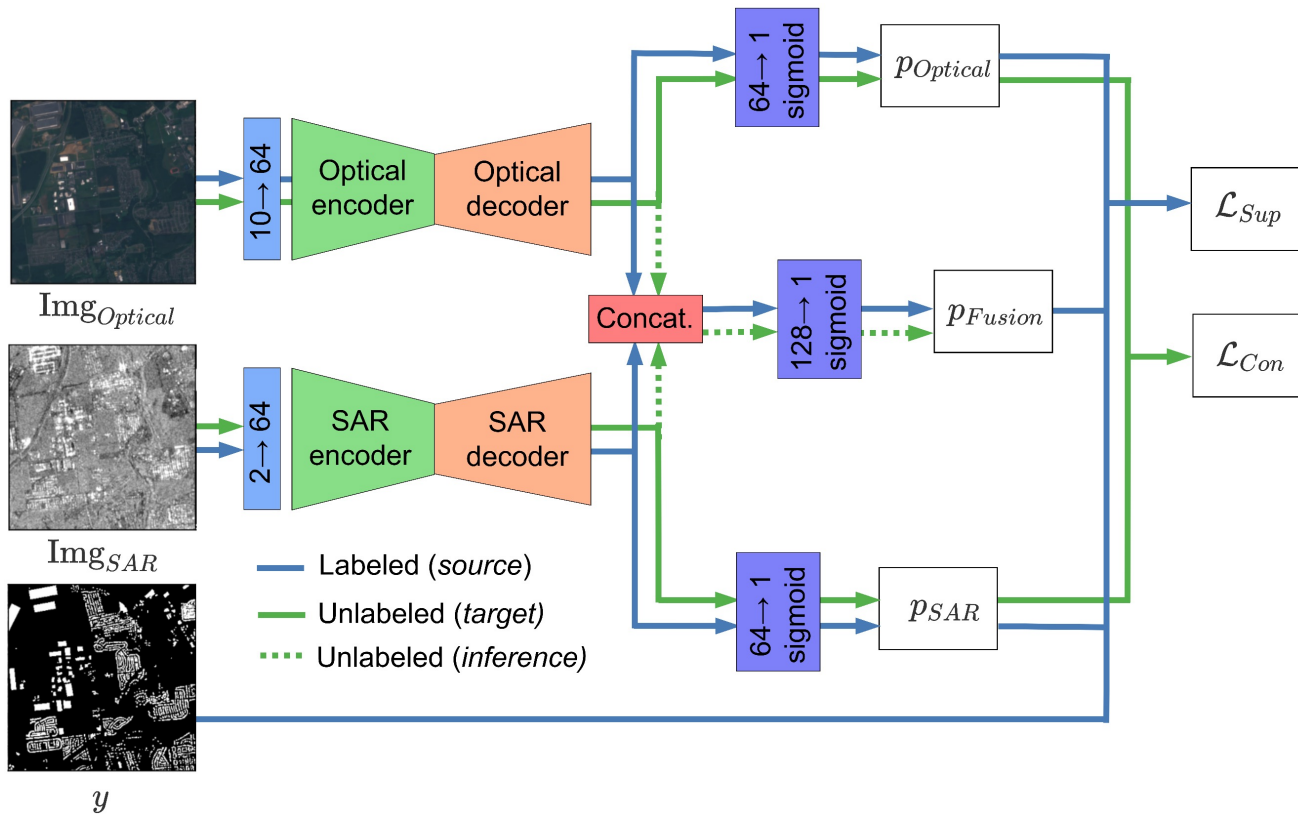
Urban mapping



Urban change detection



Overview of Fusion-DA approach

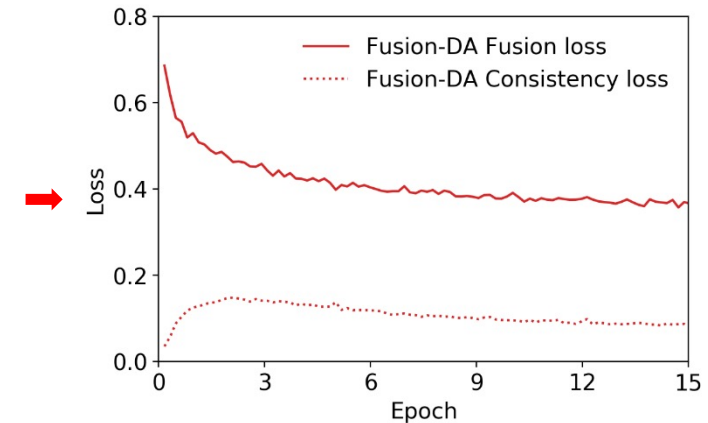


Self-supervised training

$$\mathcal{L}_{Sup} = \mathcal{L}_{pJacc}(p_{SAR}, y) + \mathcal{L}_{pJacc}(p_{Optical}, y) + \mathcal{L}_{pJacc}(p_{Fusion}, y)$$

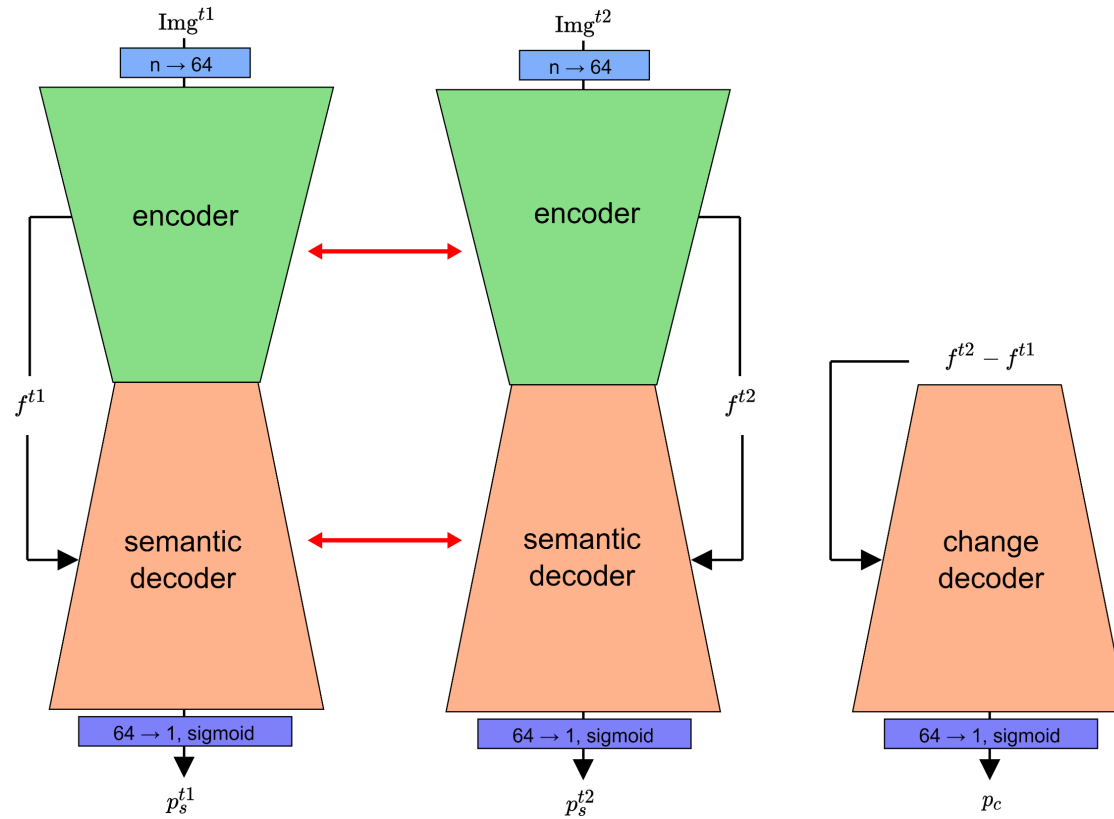
$$\mathcal{L}_{Con} = \mathcal{L}_{pJacc}(p_{Optical}, p_{SAR})$$

$$\rightarrow \mathcal{L}_{sample} = \begin{cases} \mathcal{L}_{Sup}, & \text{if } y \text{ exists} \\ \varphi \cdot \mathcal{L}_{Con}, & \text{otherwise} \end{cases}$$



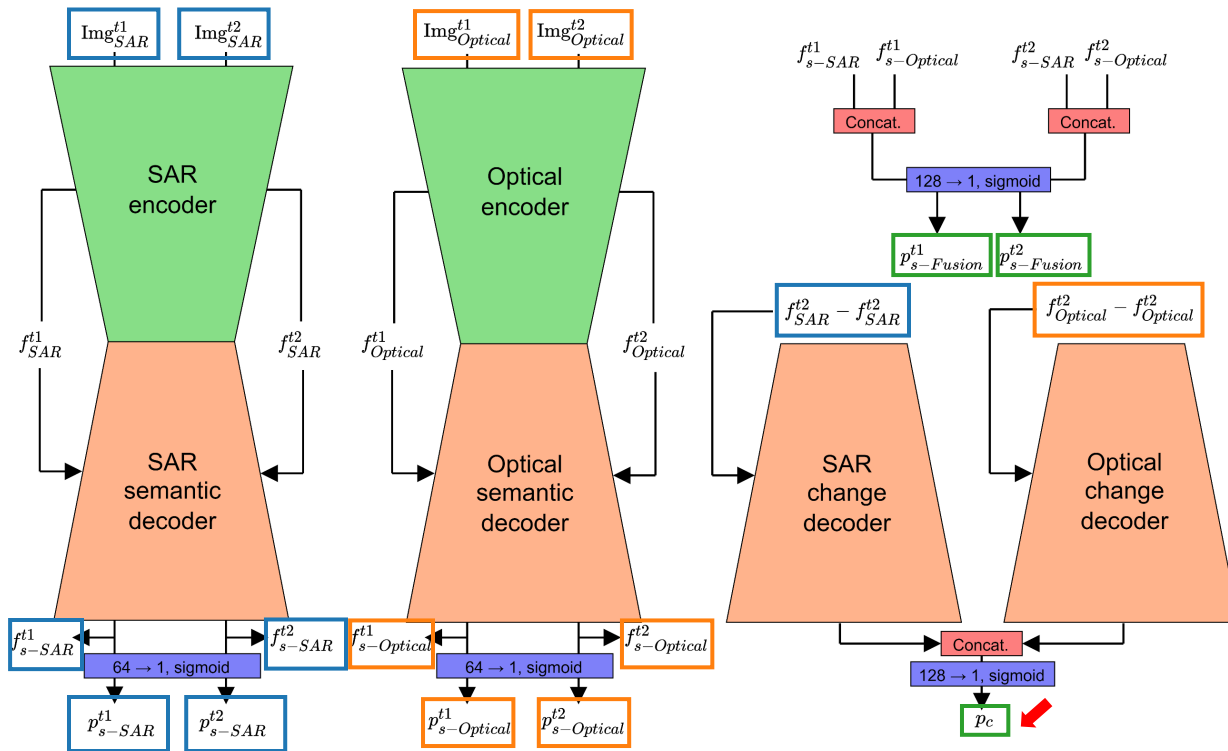
Hafner, S., Y. Ban, and A. Nascetti. 2022. Unsupervised Domain Adaptation for Global Urban Extraction using Sentinel-1 and Sentinel-2 Data. *Remote Sensing of Environment*, Volume 280, 113192, <https://doi.org/10.1016/j.rse.2022.113192>.

Siam-Diff Dual-Task U-Net



Hafner, S., A. Nascetti, H. Azizpour and Y. Ban. 2021. Sentinel-1 and Sentinel-2 Data Fusion for Urban Change Detection using a Dual Stream U-Net. *IEEE Geoscience and Remote Sensing Letters*, Vol. 19, 4019805.

Multi-Modal Siam-Diff Dual-Task



Semi-supervised training (again)

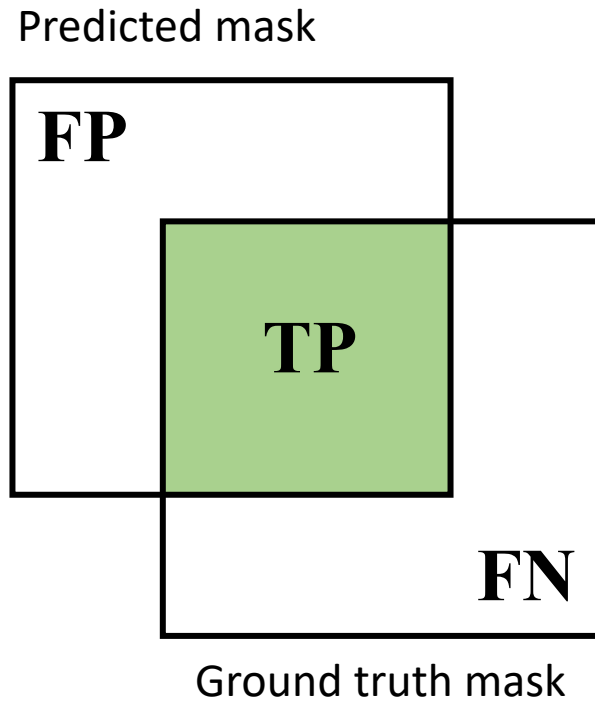
$$\mathcal{L}_c = \mathcal{L}_{pJacc}(p_c, y_c)$$

$$\mathcal{L}_s = \mathcal{L}_{pJacc}(p_{s-SAR}^{t1}, y_s^{t1}) + \mathcal{L}_{pJacc}(p_{s-SAR}^{t2}, y_s^{t2}) + \mathcal{L}_{pJacc}(p_{s-Optical}^{t1}, y_s^{t1}) + \mathcal{L}_{pJacc}(p_{s-Optical}^{t2}, y_s^{t2}) + \mathcal{L}_{pJacc}(p_{s-Fusion}^{t1}, y_s^{t1}) + \mathcal{L}_{pJacc}(p_{s-Fusion}^{t2}, y_s^{t2})$$

$$\mathcal{L}_{cons} = \mathcal{L}_{L2}(p_{s-SAR}^{t1}, p_{s-Optical}^{t1}) + \mathcal{L}_{L2}(p_{s-SAR}^{t2}, p_{s-Optical}^{t2})$$

$$\mathcal{L}_{sample} = \begin{cases} \alpha \cdot (\mathcal{L}_c + \mathcal{L}_s), & \text{if } y \text{ exists} \\ (1 - \alpha) \cdot \mathcal{L}_{cons}, & \text{otherwise} \end{cases}$$

 SAR
 Optical
 Fusion

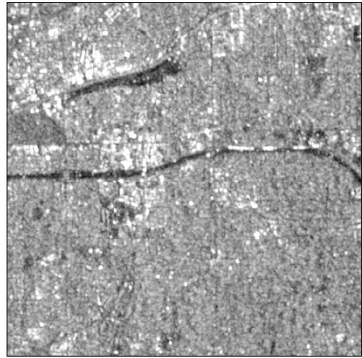


$$\text{F1 score} = \frac{\text{TP}}{\text{TP} + \frac{1}{2}(\text{FP} + \text{FN})}$$

$$\text{precision} = \frac{\text{TP}}{\text{TP} + \text{FP}}$$

$$\text{recall} = \frac{\text{TP}}{\text{TP} + \text{FN}}$$

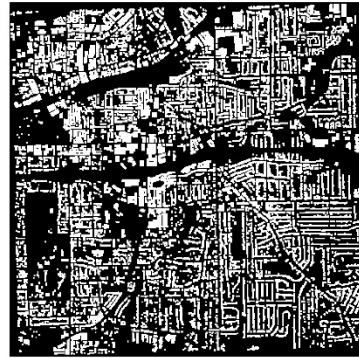
$$\text{IoU} = \frac{\text{TP}}{\text{TP} + \text{FP} + \text{FN}}$$



(a) SAR (VV)



(b) Optical (True Color)



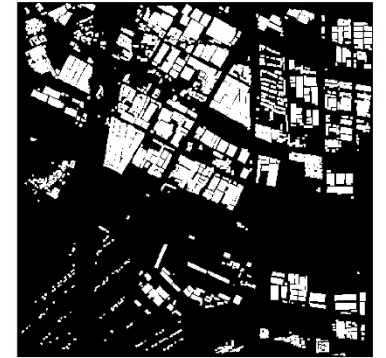
(c) SpaceNet7 Ground Truth



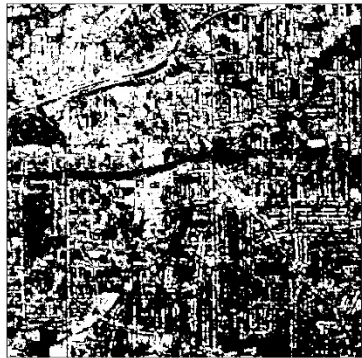
(a) SAR (VV)



(b) Optical (True Color)



(c) SpaceNet7 Ground Truth



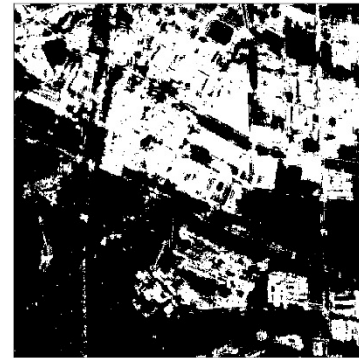
(d) GHS-S2



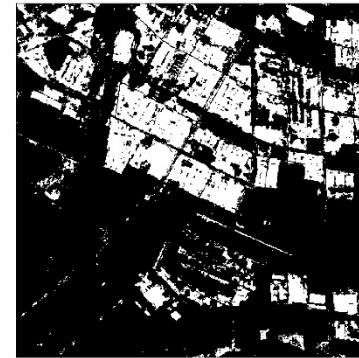
(e) WSF2019



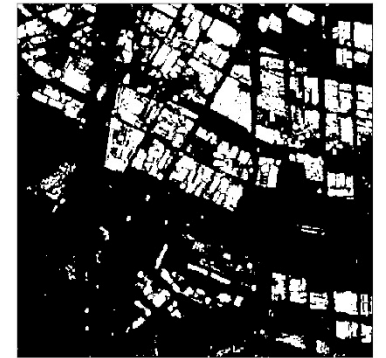
(f) Ours (Fusion-DA)



(d) GHS-S2



(e) WSF2019



(f) Ours (Fusion-DA)





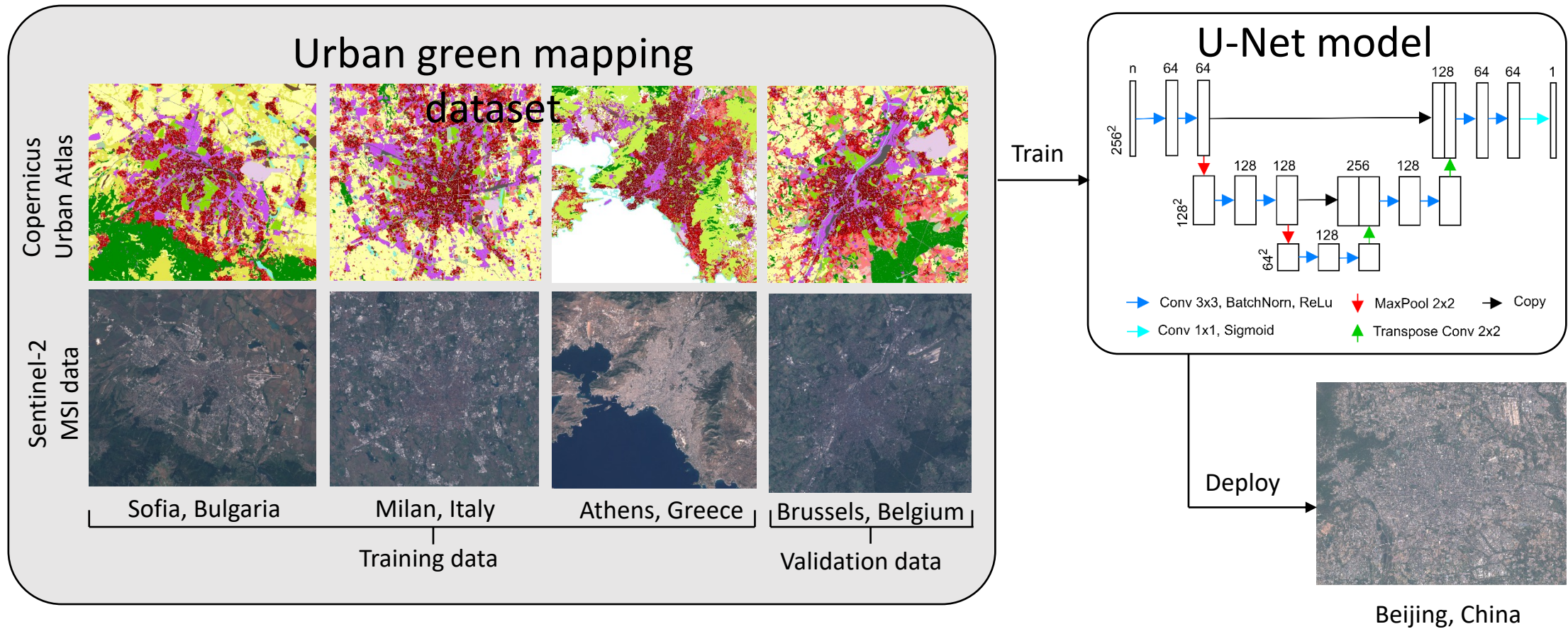
Dar Es Salaam

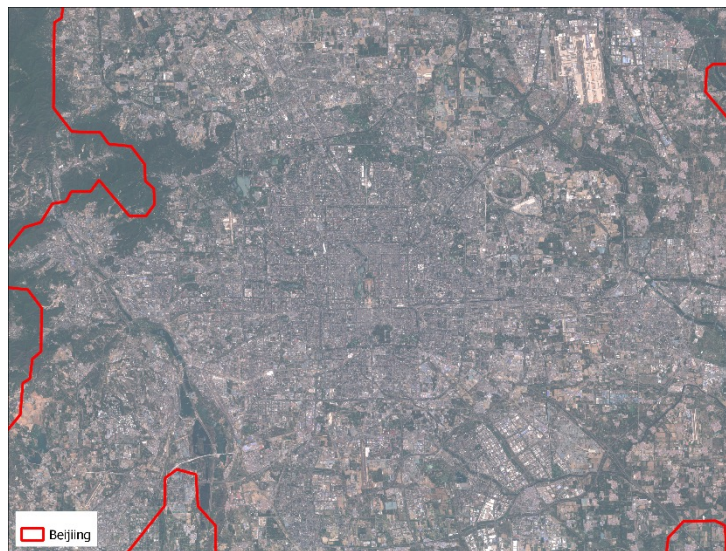


KTH



GHS-S2

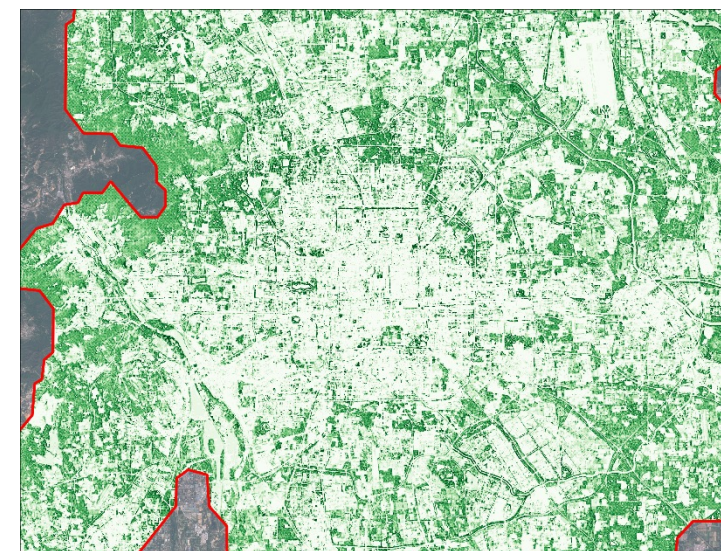




Sentinel-2 MSI scene



NDVI-based urban green map



Deep learning-based urban green map

Preliminary results:

1. NDVI-based map is noisier and overestimates urban green area
2. Deep learning model does not require local threshold adjustments

Current challenges:

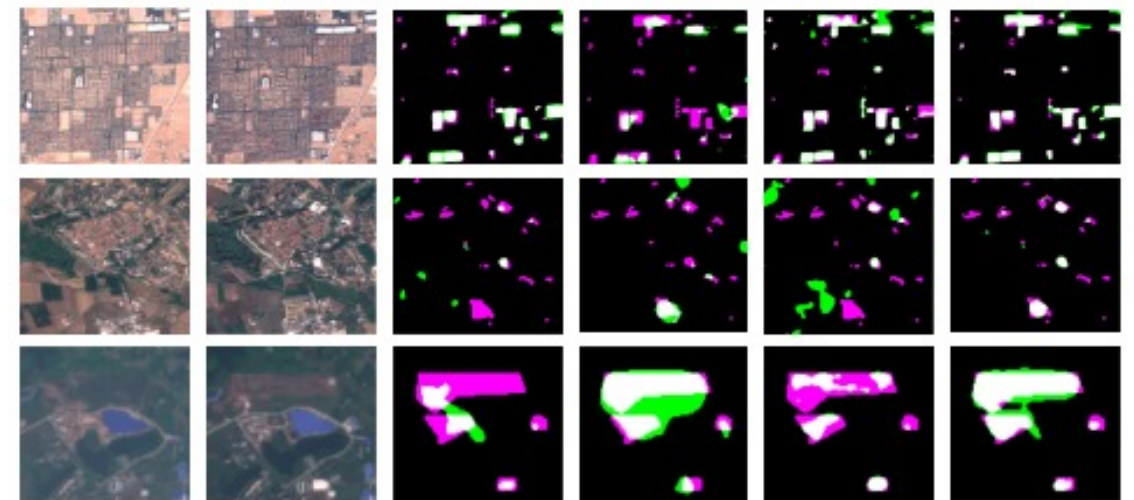
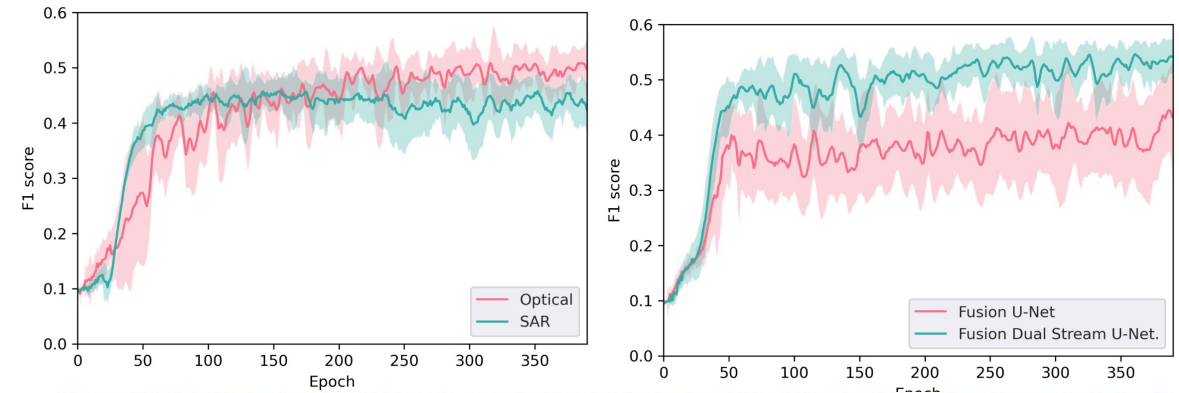
1. A clear definition of urban green is required
2. Training robust deep learning models requires a lot of training data

- Optical network outperforms SAR network
- But SAR is better in some cases
- Decision-level fusion performs better than input-level fusion
- Dual Stream U-Net achieves state-of-the-art performance on OSCD dataset

Network	Input	Precision	Recall	F1 score	F1 score ($\mu \pm \sigma$)
Siam-Diff	Optical	0.578	0.580	0.579	-
Our U-Net	Optical	0.536	0.544	0.540	0.502 \pm 0.048
Our U-Net	SAR	0.537	0.433	0.480	0.432 \pm 0.042
Our U-Net	Fusion	0.550	0.560	0.555	0.435 \pm 0.097
Our DS U-Net	Fusion	0.687	0.532	0.600	0.542 \pm 0.033

Hafner, S., A. Nascetti, H. Azizpour and Y. Ban. 2021. Sentinel-1 and Sentinel-2 Data Fusion for Urban Change Detection using a Dual Stream U-Net. *IEEE Geoscience and Remote Sensing Letters*, Vol. 19, 4019805.

2023-10-05



S2 t1

S2 t2

Optical U-Net

SAR U-Net

Fusion U-Net

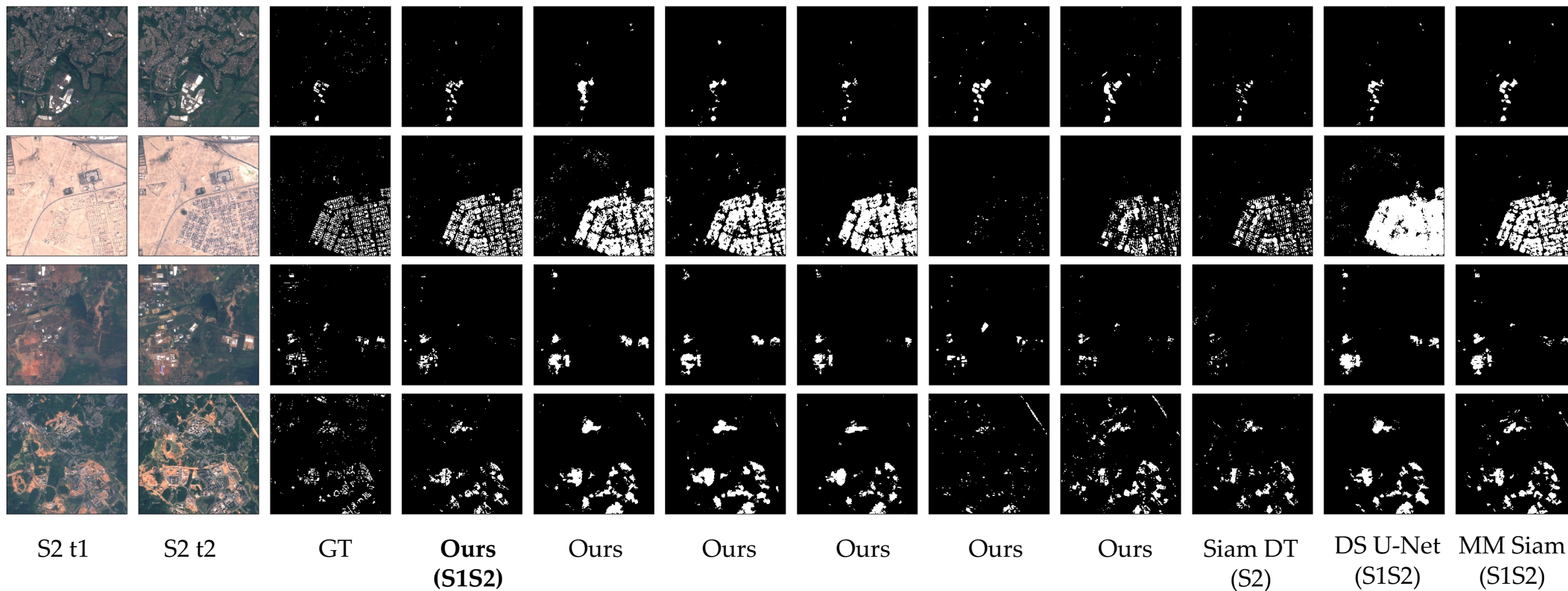
Fusion DS U-net

Urban change detection

Input	Network	F1 score	Precision	Recall
S1	U-Net EF	0.351 ± 0.008	0.326 ± 0.039	0.397 ± 0.066
	Siam-Diff	0.348 ± 0.010	0.307 ± 0.031	0.414 ± 0.056
	Siam-Diff DT	0.356 ± 0.011	0.357 ± 0.027	0.361 ± 0.042
S2	U-Net EF	0.107 ± 0.025	0.410 ± 0.047	0.063 ± 0.019
	Siam-Diff	0.252 ± 0.070	0.406 ± 0.072	0.213 ± 0.103
	Siam-Diff DT	0.301 ± 0.038	0.494 ± 0.052	0.222 ± 0.048
S1S2	DS U-Net	0.315 ± 0.054	0.386 ± 0.106	0.332 ± 0.136
	MM Siam-Diff	0.424 ± 0.013	0.446 ± 0.041	0.415 ± 0.060
	MMCR (<i>ours</i>)	0.444 ± 0.016	0.474 ± 0.040	0.425 ± 0.048

Urban mapping

Input	Network	F1 score	Precision	Recall
S1	Siam-Diff DT	0.537 ± 0.031	0.544 ± 0.025	0.540 ± 0.083
S2	Siam-Diff DT	0.562 ± 0.013	0.553 ± 0.015	0.574 ± 0.039
S1S2	MMCR (<i>ours</i>)	0.571 ± 0.039	0.617 ± 0.024	0.540 ± 0.088



Urban mapping

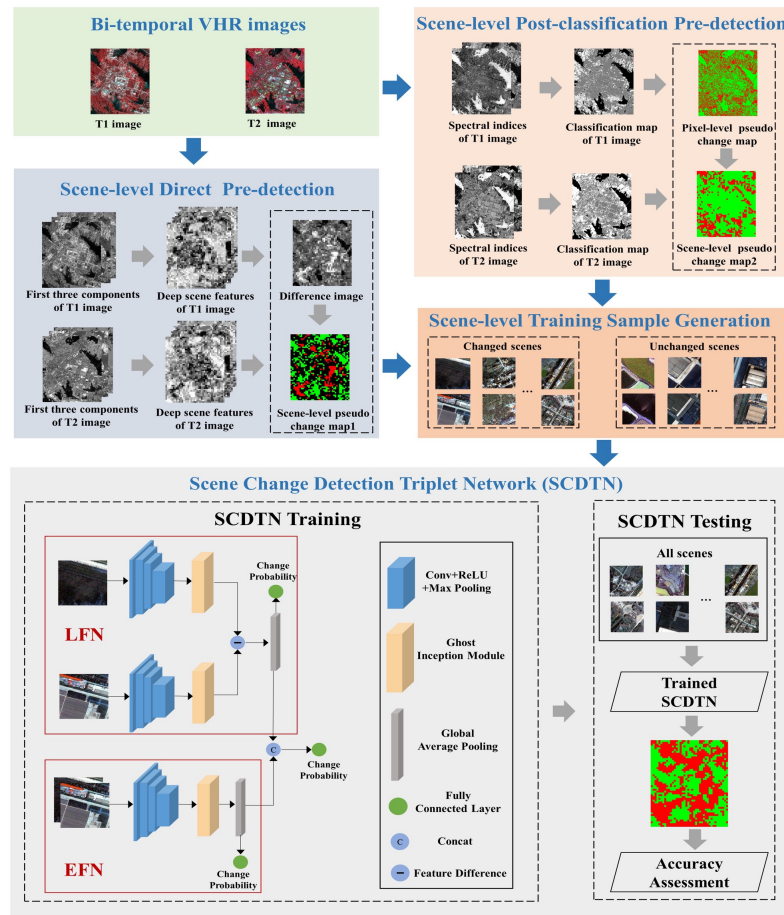
perform poorly when encountering domain shifts in satellite data

- Unlabeled multi-modal satellite data can be exploited to improve across-region generalization ability of networks
- Unsupervised domain adaptation has the potential to train robust and accurate models for global urban mapping

Urban change detection

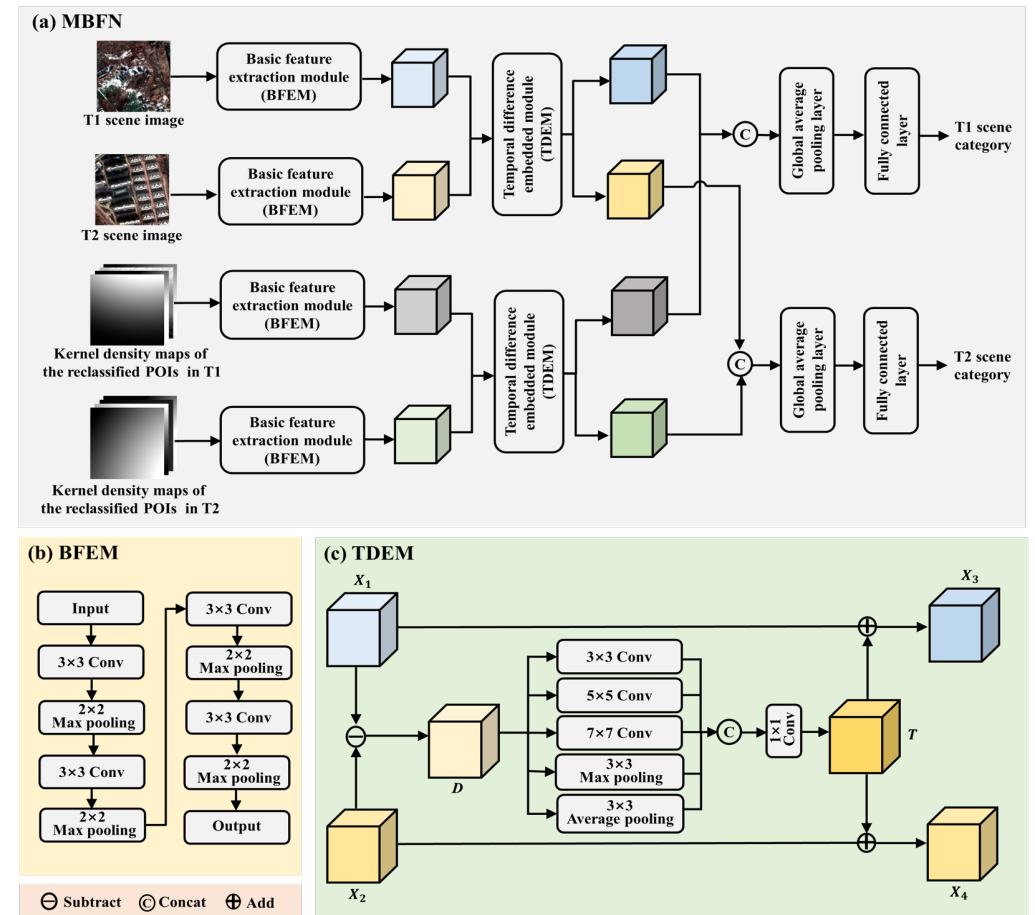
- Input-level fusion may not be sufficient to improve change detection results
- Improved change detection results can be obtained with a dual stream architecture and decision-level fusion
- Unsupervised domain adaptation is also effective for urban change detection

Automatic Urban Scene-level Binary Change Detection Based on A Novel Sample Selection Approach and Advanced Triplet Neural Network



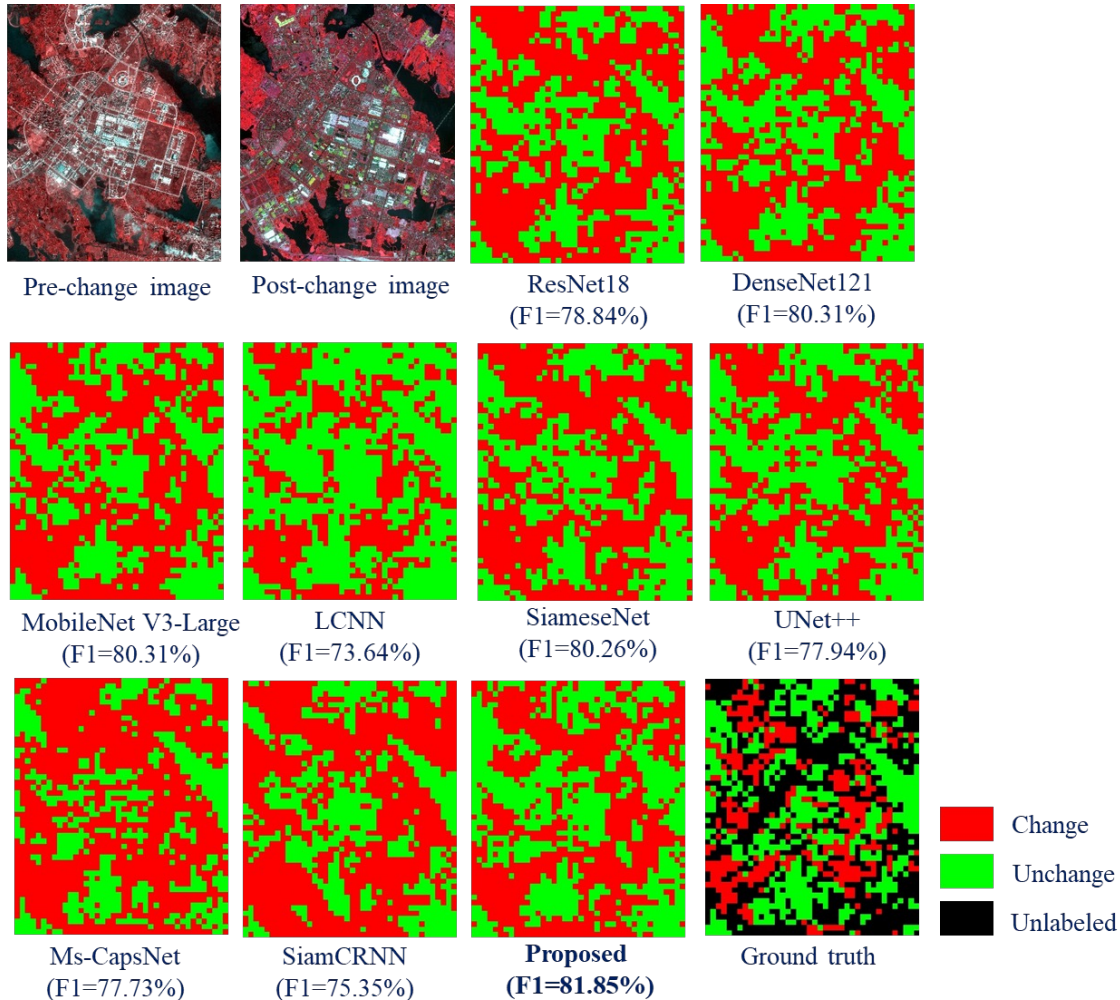
Flowchart of the proposed method

Scene-level change detection by integrating VHR images and POI data using a multiple-branch fusion network

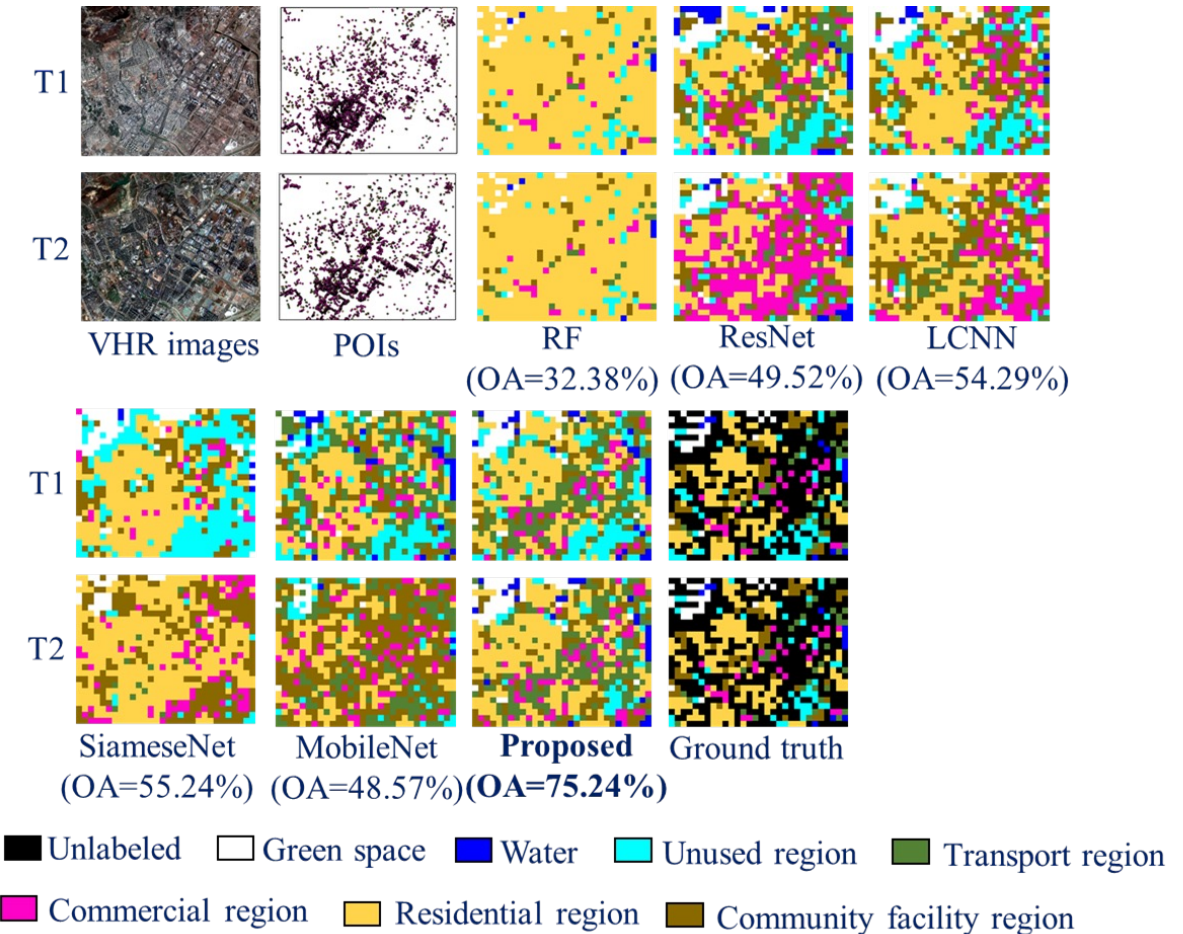


Flowchart of the proposed method

Automatic Urban Scene-level Binary Change Detection Based on A Novel Sample Selection Approach and Advanced Triplet Neural Network



Scene-level change detection by integrating VHR images and POI data using a multiple-branch fusion network



■ Automatic Urban Scene-level Binary Change Detection Based on A Novel Sample Selection Approach and Advanced Triplet Neural Network

- 1) The proposed binary scene-level change detection method outperforms some other state-of-the-art methods.
- 2) The proposed sample selection strategy can generate reliable scene-level changed and unchanged samples.
- 3) The designed triplet neural network is able to learn the deep features from each raw image and mine the temporal correlation between two raw images.

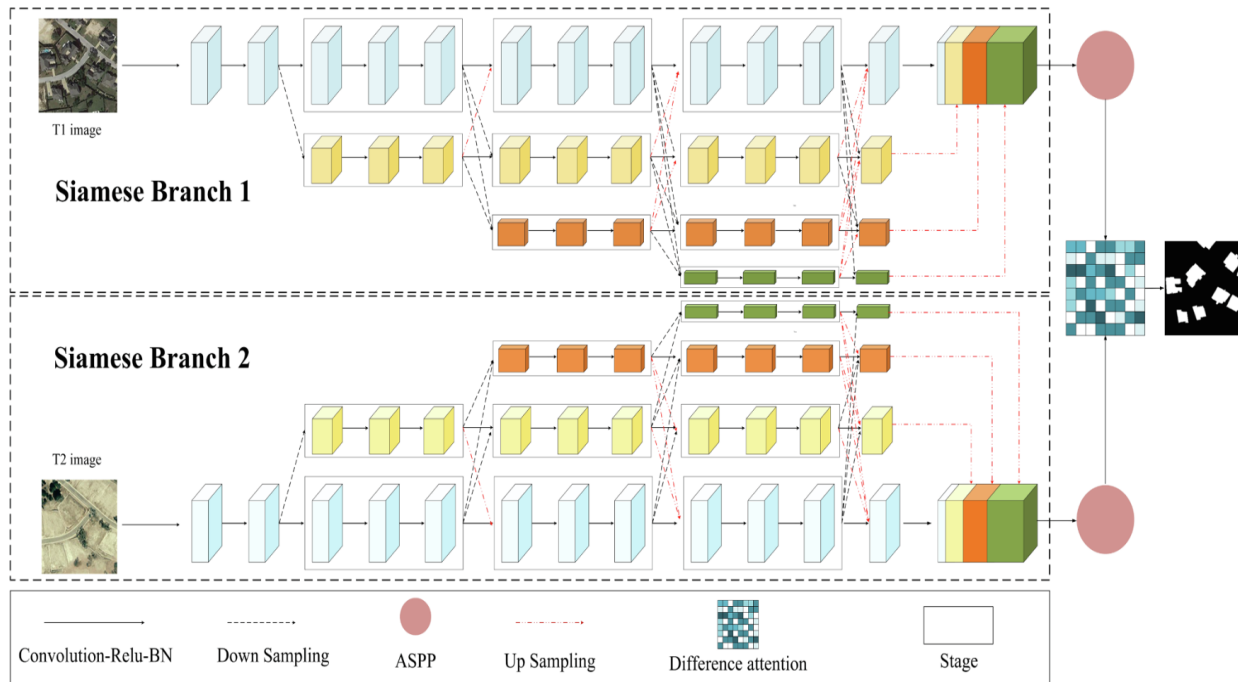
■ Scene-level change detection by integrating VHR images and POI data using a multiple-branch fusion network

- 1) The proposed scene change detection method outperforms some other state-of-the-art methods.
- 2) Using both VHR images and POIs as inputs to the network can guarantee the comprehensive extraction of information.
- 3) The proposed temporal difference embedded module can effectively mine the temporal features between two input feature cubes.

[1] Hong Fang, Shanchuan Guo, Xin Wang, Sicong Liu, Cong Lin, **Peijun Du***. Automatic Urban Scene-Level Binary Change Detection Based on A Novel Sample Selection Approach and Advanced Triplet Neural Network. *IEEE Transactions on Geoscience and Remote Sensing*, 2023, 61, Art no. 5601518.

[2] Hong Fang, Shanchuan Guo, Cong Lin, Peng Zhang, Wei Zhang, **Peijun Du***. Scene-level change detection by integrating VHR images and POI data using a multiple-branch fusion network. *Remote Sensing Letters*, 2023, 14(8): 808-820.

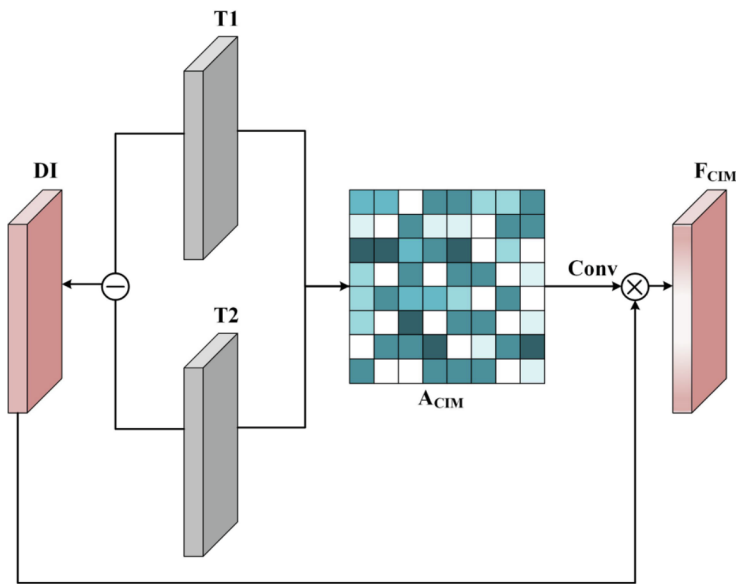
HDANet



The structure of the HDANet framework

- HDANet employs a **Siamese feature discriminant** structure with shared weights to effectively extract **differential features** from two distinct time-period remote sensing images.
- Integrating the feature representation with **different resolutions and scales in parallel**, and the detailed change information is well kept for the final detection.
- Devising a differential attention module (**DAM**) based on **change intensity**, which can extract the differential features of two different temporal images effectively.

DAM module



The structure of the DAM framework

- the **Euclidean distance** between the feature map from the bi-temporal data in a pixel-wise manner is calculated to represent the **change intensity map (CIM)**. Convolution is implemented on the change intensity map, which can generate the **difference attention weights**.

$$CIM = \sqrt{\sum_{c=1}^n (T_{1c} - T_{2c})^2}$$

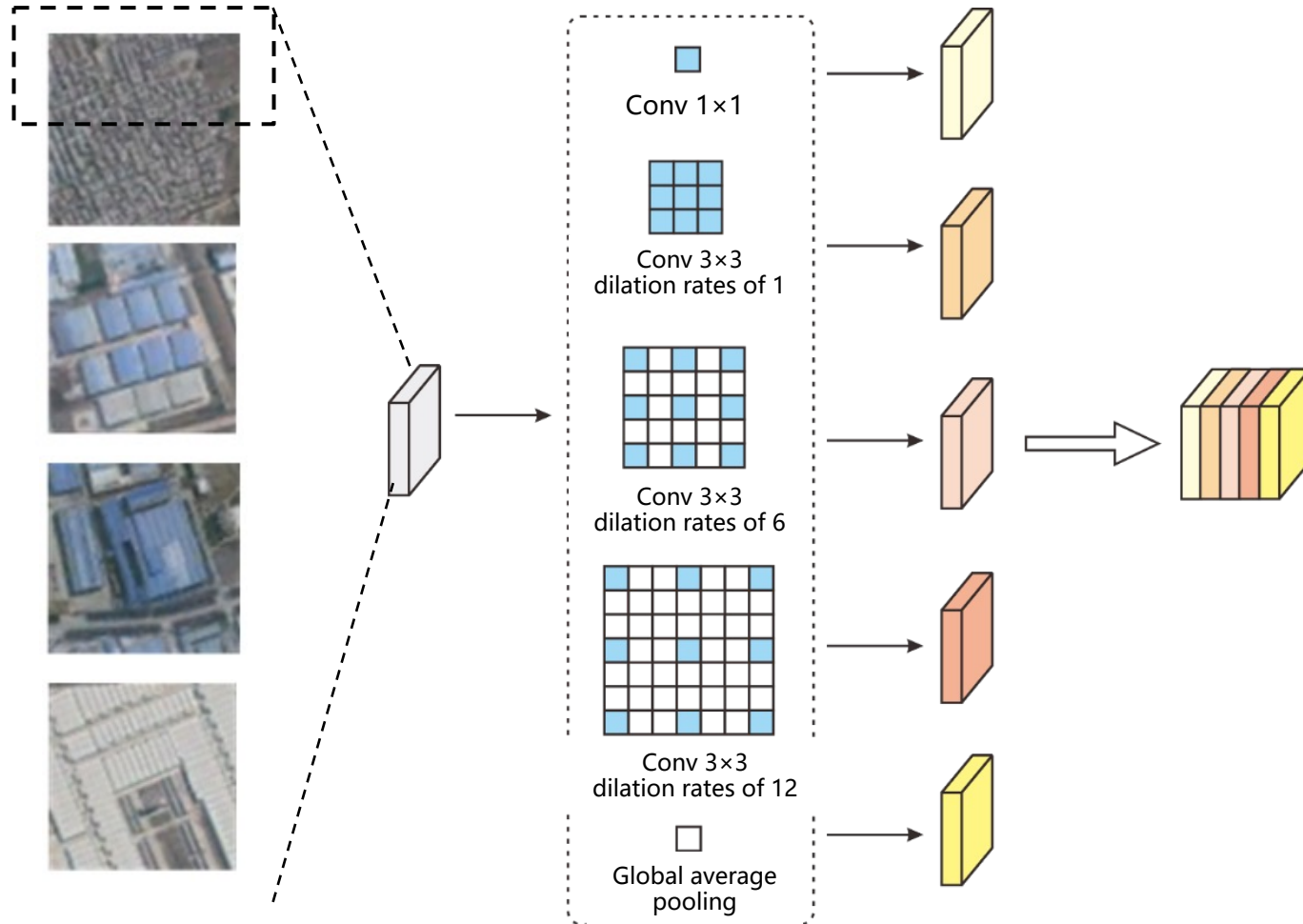
$$A_{CIM} = \sigma(\text{Conv}_{3 \times 3}(CIM))$$

- The **channel attention** is integrated with the **difference attention weight** to obtain the output attention.

$$DI = |T_1 - T_2|$$



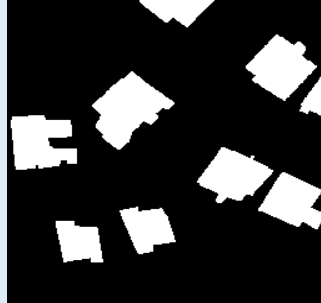
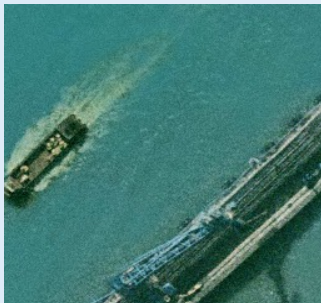
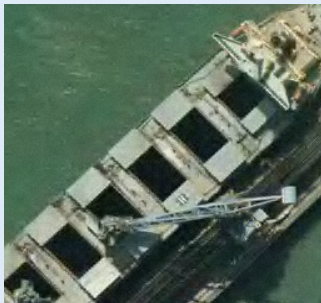


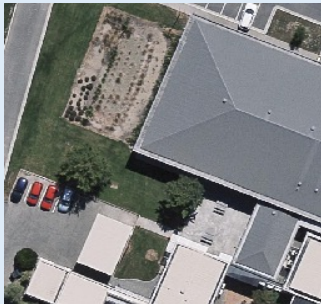
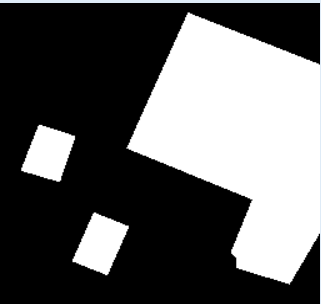
$$F_{CIM} = A_{CIM} \otimes DI$$

ASPP module



- ASPP employs parallel atrous convolutional layers with **different dilation rates** to capture **both local and global context** from images, which enhances the contextual understanding of images.
- ASPP is appended after the Siamese high-resolution feature extraction for the **multi-scale feature** learning, which can learn the **difference information**.

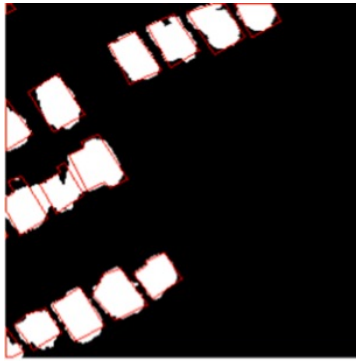
Running on the GeForce RTX 3090 GPU with Image size as 256×256 , and batch size as 4.

Dataset	Number	T1	T2	Reference
LEVIR-CD	train: 7120 eval: 1024 test: 2048			
SYSU-CD	train: 12000 eval: 4000 test: 4000			
WHU-building	train: 5948 eval: 743 test: 743			

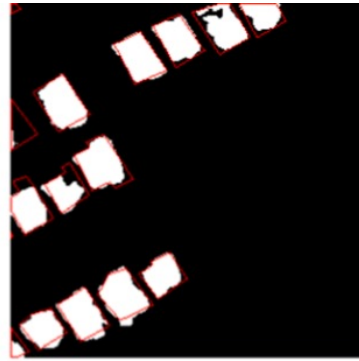
LEVIR-CD



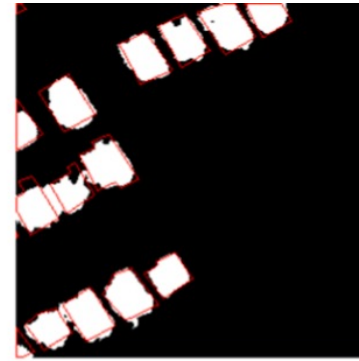
T1



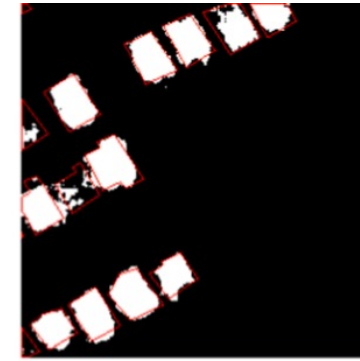
FC_EF



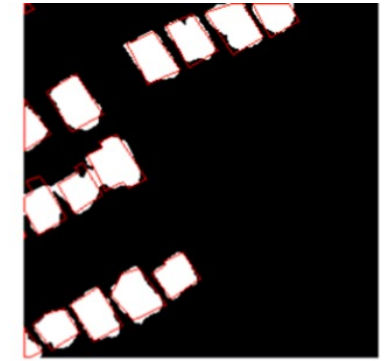
FC_Siam_conc



FC_Siam_diff



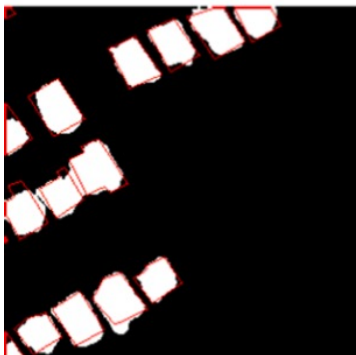
SegNet



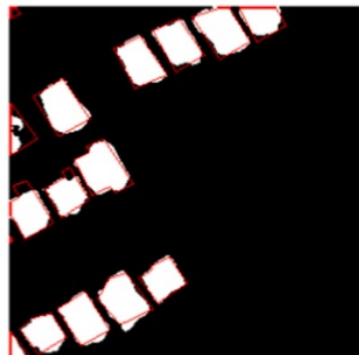
Deeplab



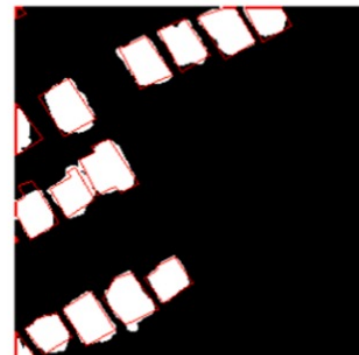
T2



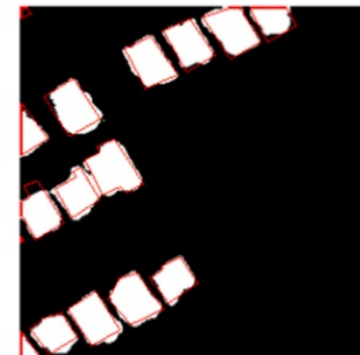
DSIFN



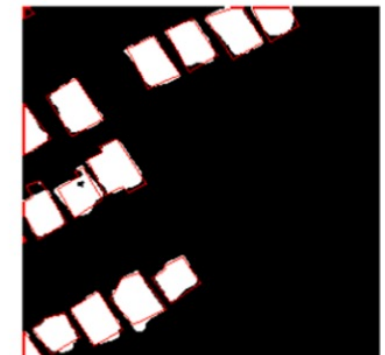
STANet



Unet++

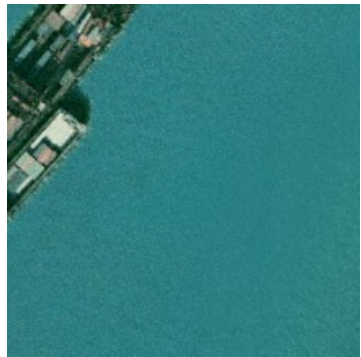


Siam_HRNet



HDANet

SYSU-CD



T1



FC_EF



FC_Siam_conc



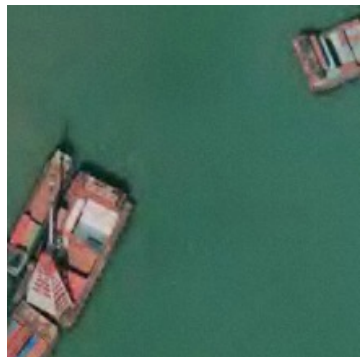
FC_Siam_diff



SegNet



Deeplab



T2



DSIFN



STANet



Unet++



Siam_HRNet

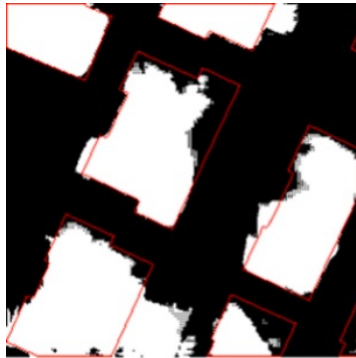


HDANet

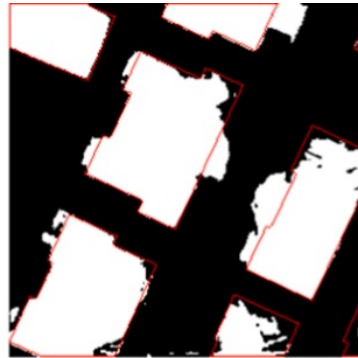
WHU-building



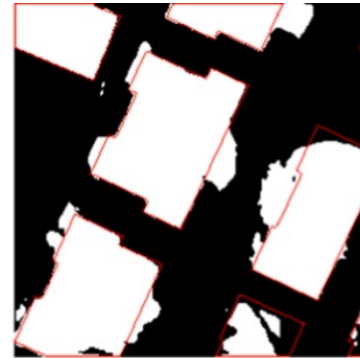
T1



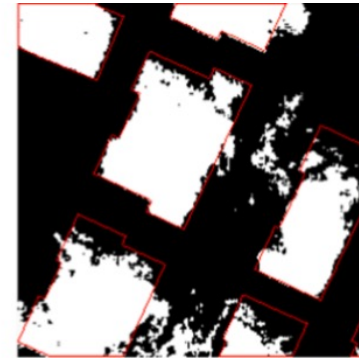
FC_EF



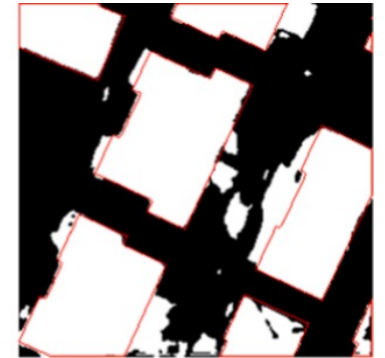
FC_Siam_conc



FC_Siam_diff



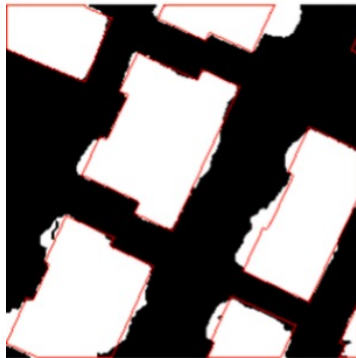
SegNet



Deeplab



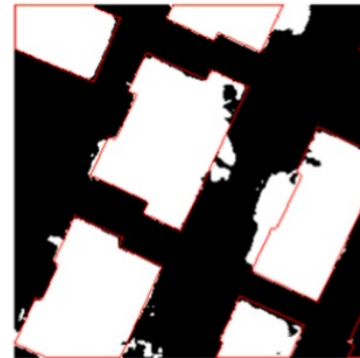
T2



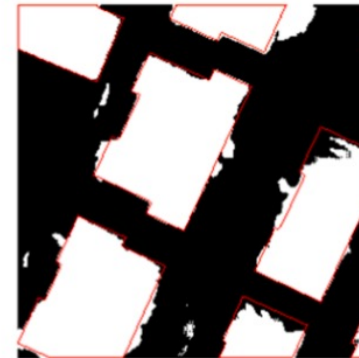
DSIFN



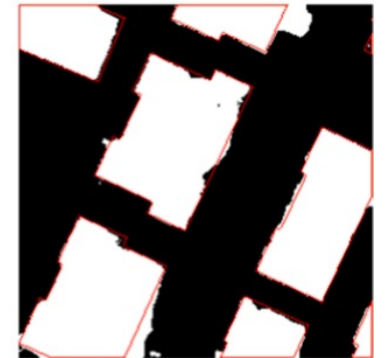
STANet



Unet++



Siam_HRNet



HDANet

The accuracy of the different approaches for the LEVIR-CD dataset

Methods	Precision	Recall	F1	Kappa
FC_EF	0.9016	0.7255	0.8040	0.7947
FC_Siam_conc	0.9394	0.7597	0.8401	0.8324
FC_Siam_diff	0.8911	0.7756	0.8293	0.8209
SegNet	0.9247	0.7094	0.8029	0.7938
DeepLab V3	0.9003	0.8251	0.8611	0.8539
DSIFN	0.9278	0.8211	0.8712	0.8647
STANet	0.9201	0.8333	0.8746	0.8682
Unet+ +	0.9144	0.8524	0.8823	0.8762
Siam_HRNet	0.9108	0.8479	0.8782	0.8719
HDANet	0.9226	0.8761	0.8987	0.8934

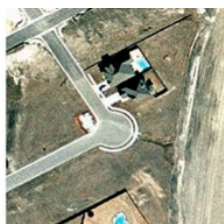
The accuracy of the different approaches for the SYSU-CD dataset

Methods	Precision	Recall	F1	Kappa
FC_EF	0.8269	0.6308	0.7156	0.6427
FC_Siam_conc	0.7792	0.7208	0.7488	0.6752
FC_Siam_diff	0.8492	0.6430	0.7319	0.6635
SegNet	0.8235	0.6629	0.7345	0.6638
DeepLab V3	0.8099	0.7065	0.7547	0.6856
DSIFN	0.7932	0.7285	0.7595	0.6894
STANet	0.8038	0.7475	0.7746	0.7084
Unet+ +	0.8144	0.7466	0.7790	0.7146
Siam_HRNet	0.8095	0.7391	0.7727	0.7066
HDANet	0.7853	0.7988	0.7920	0.7271

The accuracy of the different approaches for the WHU-building dataset

Methods	Precision	Recall	F1	Kappa
FC_EF	0.7623	0.7765	0.7693	0.7603
FC_Siam_conc	0.8831	0.7261	0.7969	0.7899
FC_Siam_diff	0.8020	0.7631	0.7821	0.7739
SegNet	0.7813	0.6878	0.7316	0.7219
DeepLab V3	0.8256	0.8197	0.8226	0.8158
DSIFN	0.8686	0.8093	0.8379	0.8319
STANet	0.8601	0.8340	0.8468	0.8410
Unet+ +	0.8906	0.7898	0.8372	0.8313
Siam_HRNet	0.8806	0.8098	0.8437	0.8380
HDANet	0.8987	0.8255	0.8605	0.8554

LEVIR-CD



T1_original



T1_10%strip



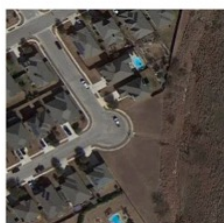
T1_50%strip



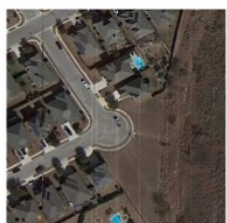
T1_10%salt



T1_50%salt



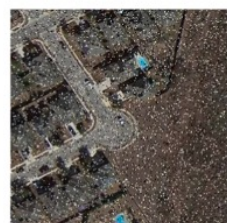
T2_original



T2_10%strip



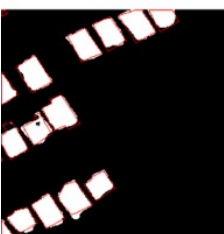
T2_50%strip



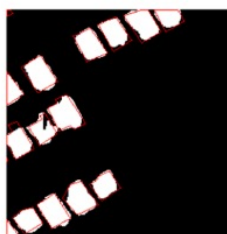
T2_10%salt



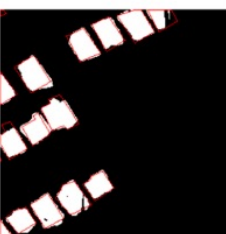
T2_50%salt



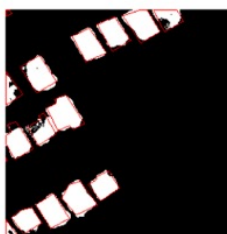
HDANet
_original



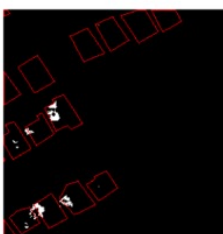
HDANet
_10%strip



HDANet
_50%strip



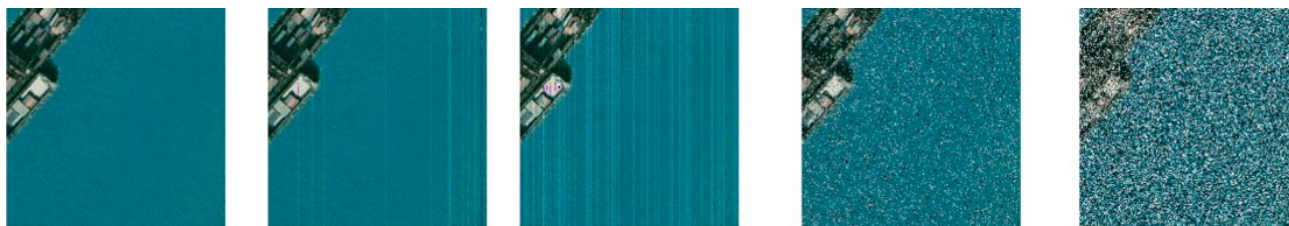
HDANet
_10%salt



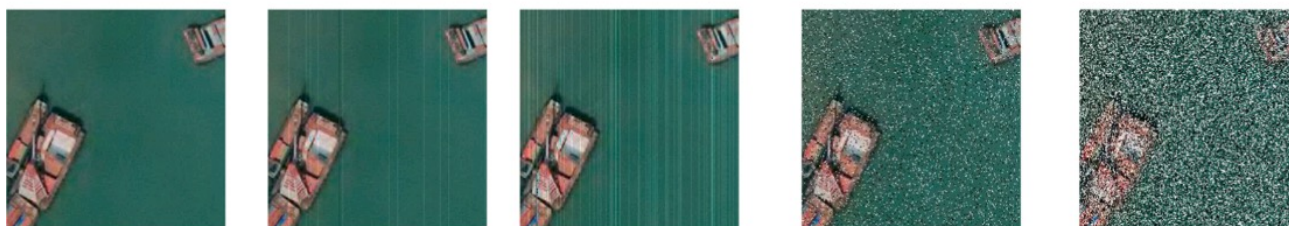
HDANet
_50%salt

Noise type	Precision	Recall	F1	Kappa
10%strip	0.8810	0.8679	0.8744	0.8635
50%strip	0.8120	0.8007	0.8063	0.7902
10%salt	0.8714	0.8795	0.8753	0.8670
50%salt	0.7834	0.7215	0.7512	0.7320

SYSU-CD



T1_original T1_10%strip T1_50%strip T1_10%salt T1_50%salt



T2_original T2_10%strip T2_50%strip T2_10%salt T2_50%salt



HDANet_original HDANet_10%strip HDANet_50%strip HDANet_10%salt HDANet_50%salt

Noise type	Precision	Recall	F1	Kappa
10%strip	0.7517	0.7342	0.7428	0.7219
50%strip	0.6829	0.6315	0.6562	0.6488
10%salt	0.7494	0.7537	0.7515	0.7371
50%salt	0.6352	0.6150	0.6249	0.6052

WHU-building



T1_original

T1_10%strip

T1_50%strip

T1_10%salt

T1_50%salt



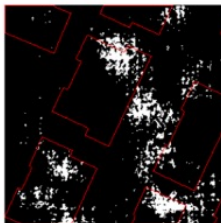
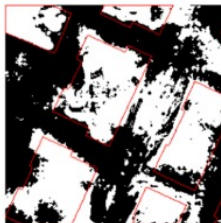
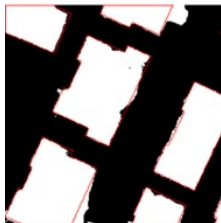
T2_original

T2_10%strip

T2_50%strip

T2_10%salt

T2_50%salt



HDANet
_original

HDANet
_10%strip

HDANet
_50%strip

HDANet
_10%salt

HDANet
_50%salt

Noise type	Precision	Recall	F1	Kappa
10%strip	0.8742	0.8681	0.8711	0.8533
50%strip	0.8251	0.8339	0.8295	0.8140
10%salt	0.8506	0.8240	0.8371	0.8219
50%salt	0.7995	0.7460	0.7718	0.7538

LEVIR-CD



Method	ASPP	DAM	CBAM	Precision	Recall	F1	Kappa
Baseline	×	×	×	0.9108	0.8479	0.8782	0.8719
Baseline+ASPP	√	×	×	0.9148	0.8537	0.8832	0.8771
Baseline+DAM	×	√	×	0.9120	0.8728	0.8920	0.8863
HDANet+CBAM	√	×	√	0.9167	0.8726	0.8941	0.8885
HDANet+DAM	√	√	×	0.9226	0.8761	0.8987	0.8934

SYSU-CD



T1



T2



Reference



Baseline



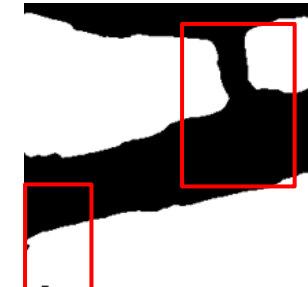
Baseline
+ASPP



Baseline
+DAM



HDANet
+CBAM



HDANet
+DAM

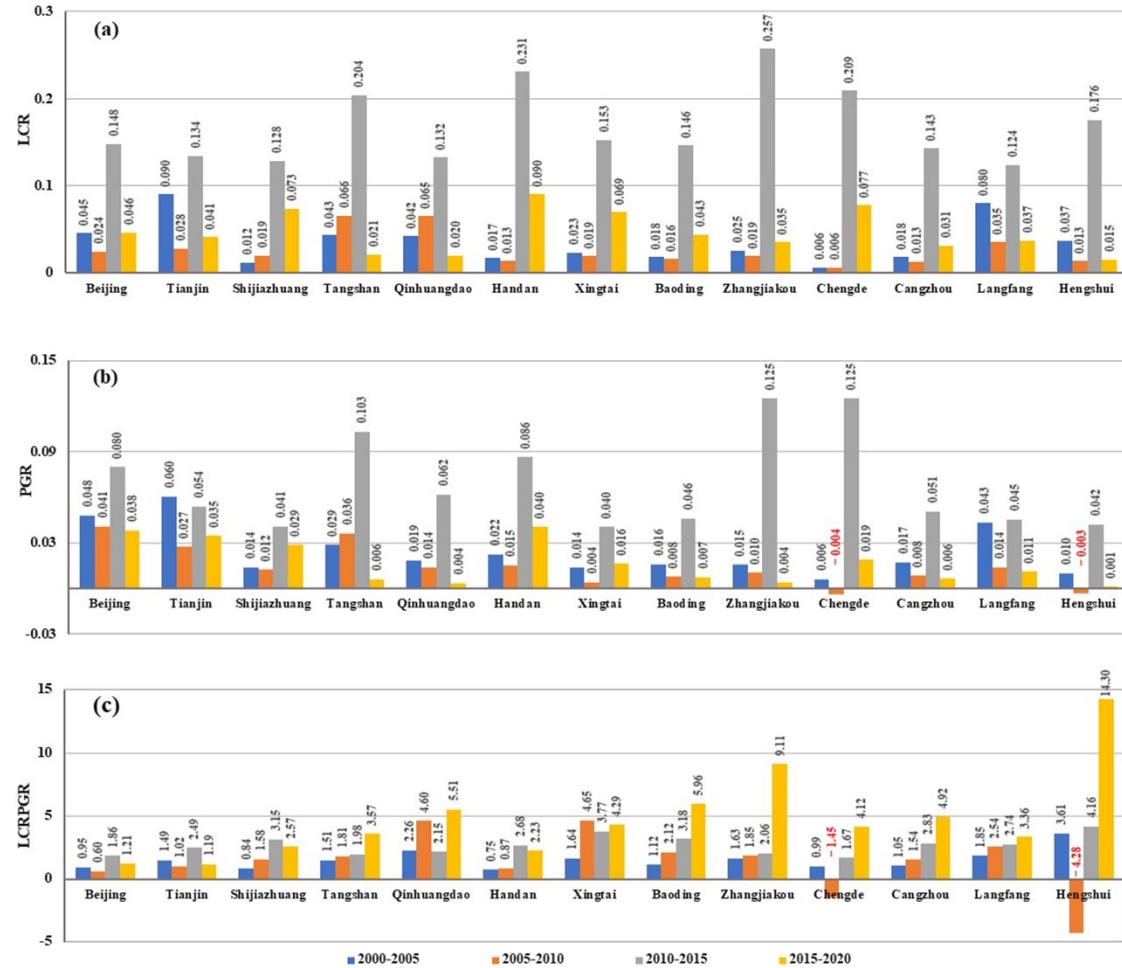
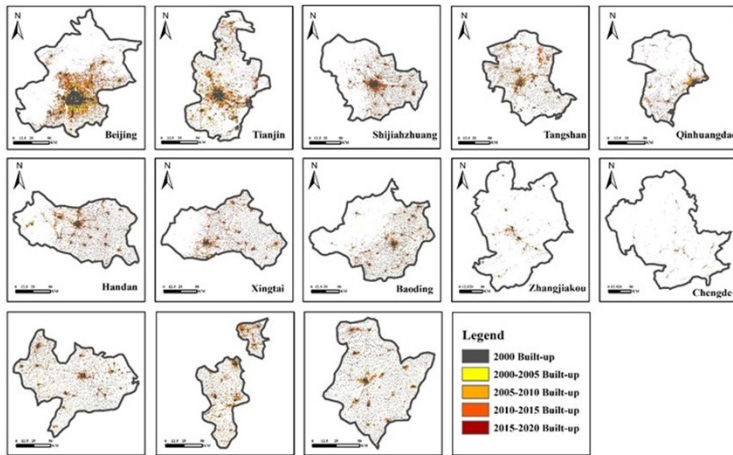
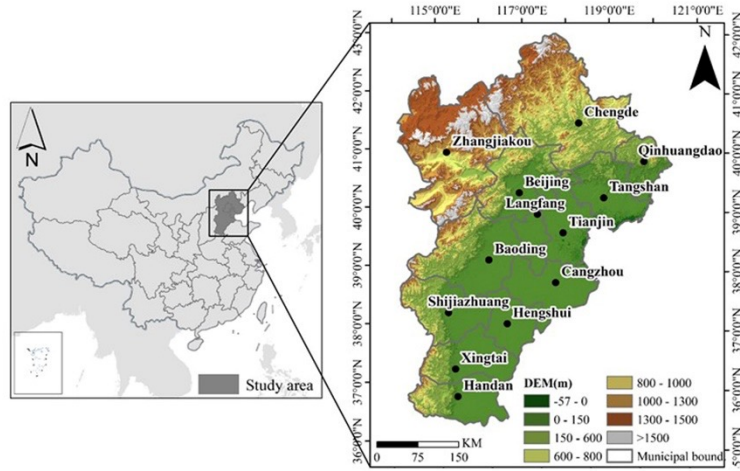
Method	ASPP	DAM	CBAM	Precision	Recall	F1	Kappa
Baseline	×	×	×	0.8095	0.7391	0.7727	0.7066
Baseline+ASPP	√	×	×	0.7955	0.7625	0.7786	0.7122
Baseline+DAM	×	√	×	0.7998	0.7678	0.7835	0.7184
HDANet+CBAM	√	×	√	0.8069	0.7635	0.7846	0.7205
HDANet+DAM	√	√	×	0.7853	0.7988	0.7920	0.7271

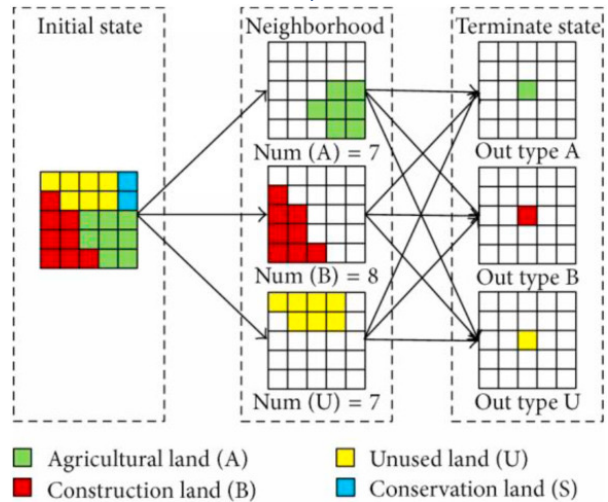
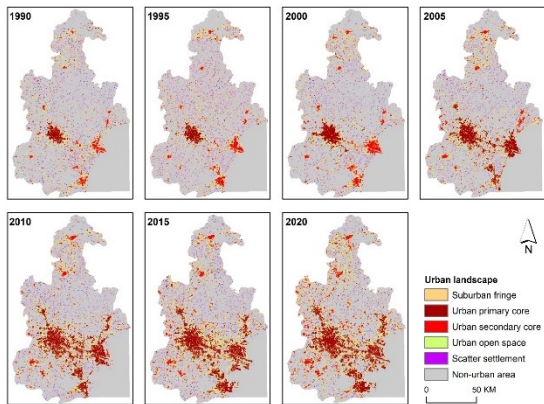
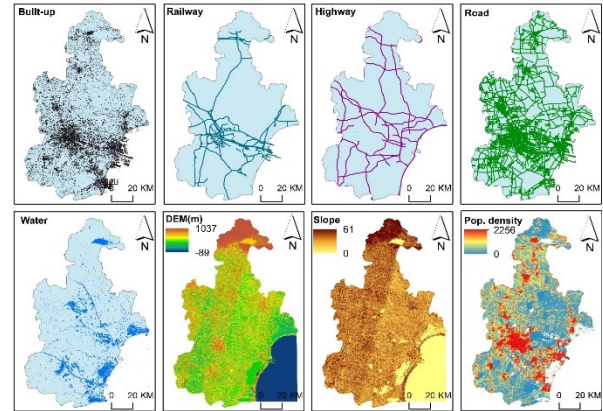
WHU-building



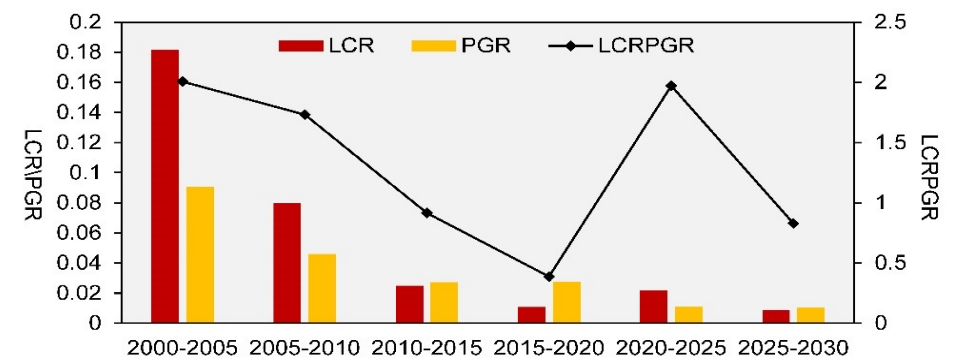
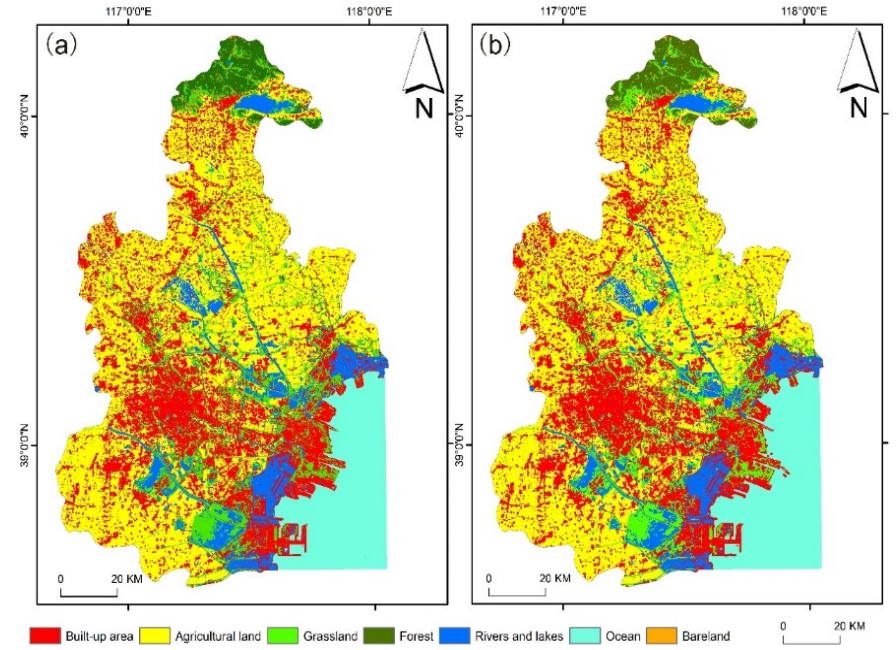
Method	ASPP	DAM	CBAM	Precision	Recall	F1	Kappa
Baseline	×	×	×	0.8806	0.8098	0.8437	0.8380
Baseline+ASPP	√	×	×	0.8899	0.8088	0.8474	0.8418
Baseline+DAM	×	√	×	0.8925	0.8171	0.8532	0.8478
HDANet+CBAM	√	×	√	0.8539	0.8559	0.8549	0.8493
HDANet+DAM	√	√	×	0.8987	0.8255	0.8605	0.8554

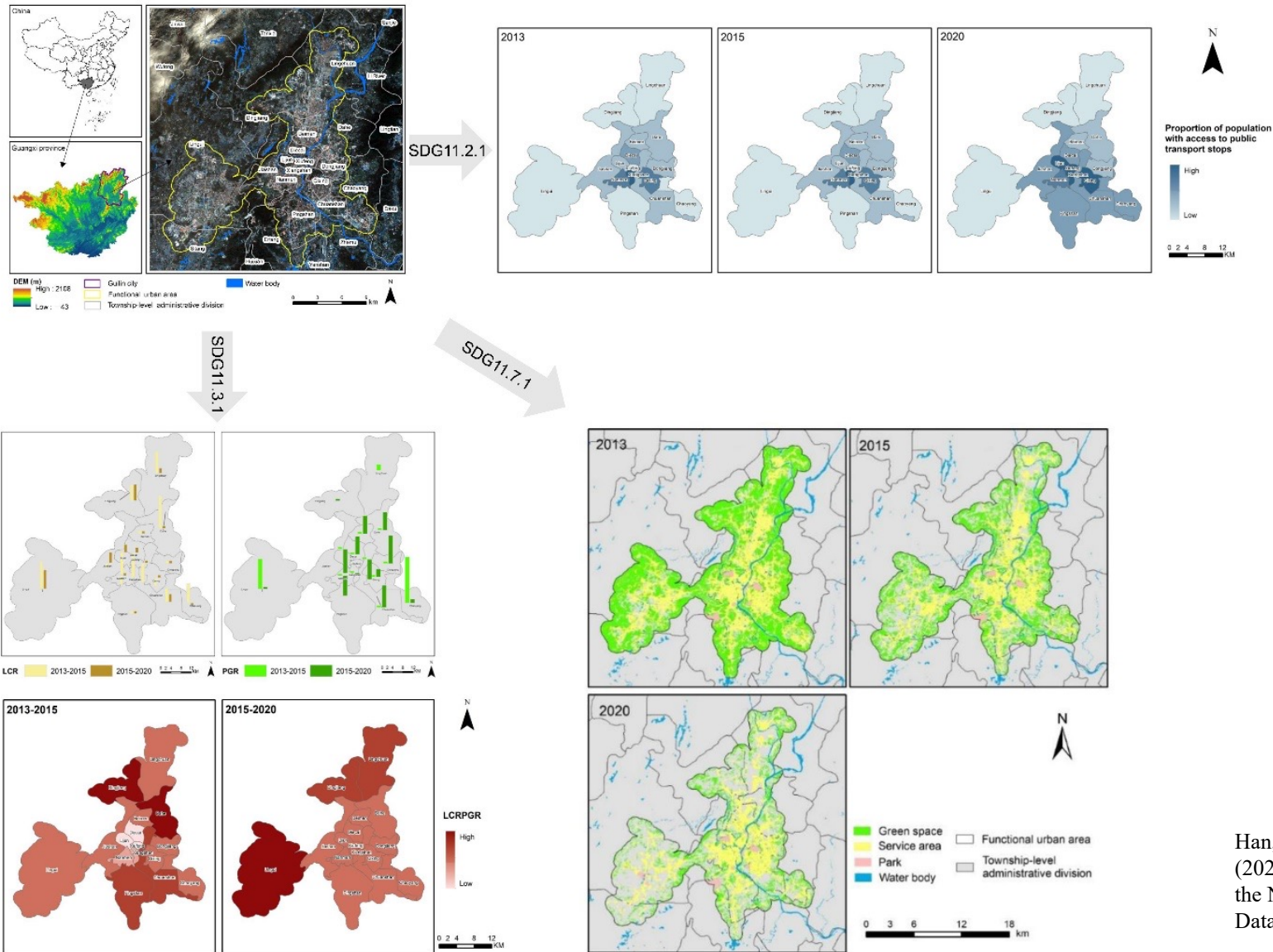
- The HDANet framework is carried out using a **Siamese network** structure with shared weights, which allows HDANet to represent the change characteristics well.
- A differential attention module based on **change intensity** is proposed to enhance the differential representation, which enhances the **differential features** of two different temporal images.
- For the case of there being land objects in the same image with different scales, the parallel ASPP module with preset dilation rates is used for the **multi-scale** features extraction.



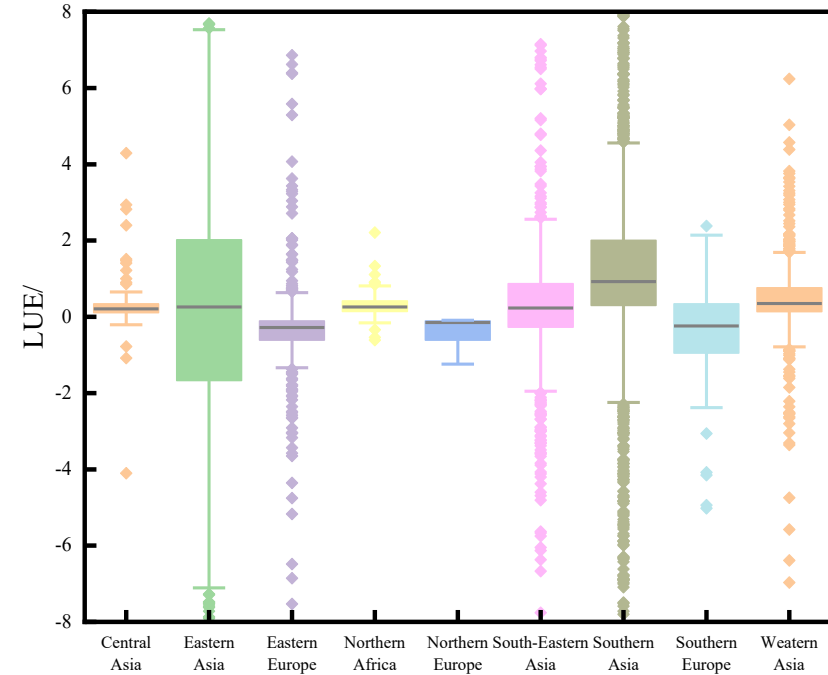
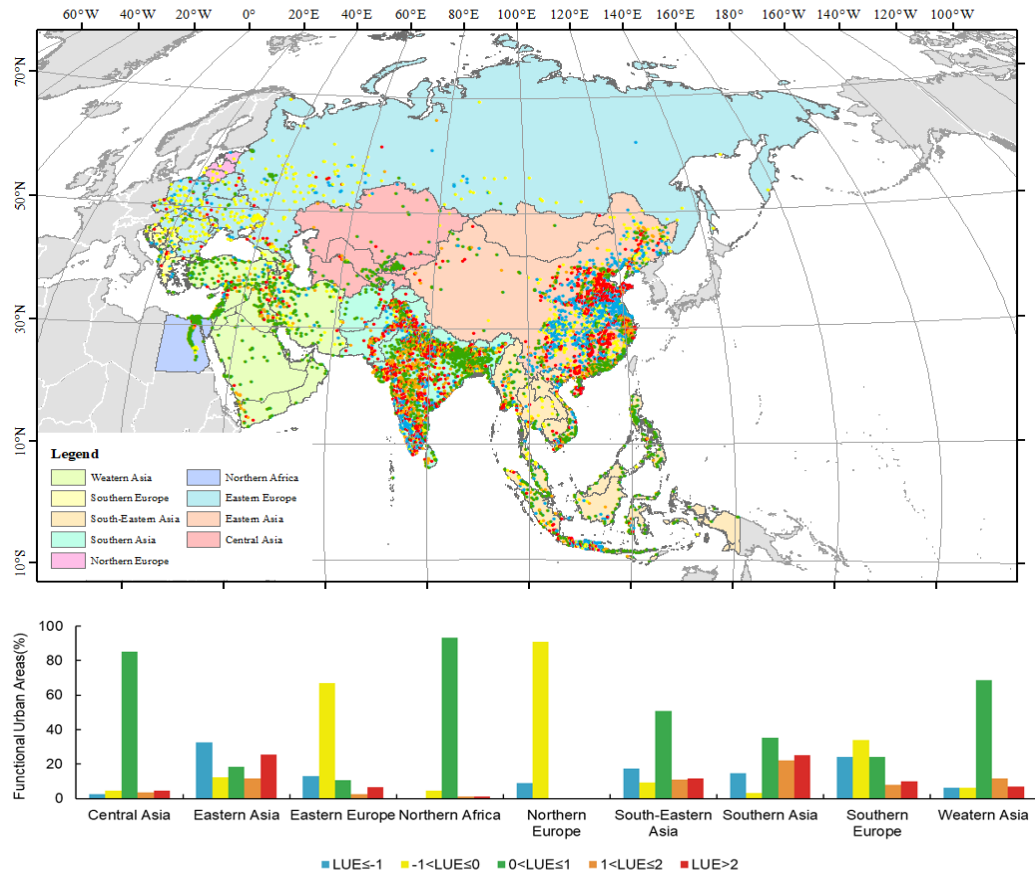


CA-Markov model





Han, L., Lu, L., Lu, J., Liu, X., Zhang, S., Luo, K., . . . Li, Q. (2022). Assessing Spatiotemporal Changes of SDG Indicators at the Neighborhood Level in Guilin, China: A Geospatial Big Data Approach. *Remote Sensing*, 14(19).



Linlin Lu, Michele Melchiorri, Sebastian Hafner, Yifang Ban, Martino Pesaresi, Muhammad Fahad Baqa, . . . Li, Q. . Big Earth data to support sustainable cities and communities in the Belt and Road region: Tools, products and application cases, International Journal of Digital Earth(to be submitted)

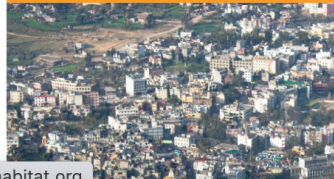


About | Contact Us

DATA TOOLS USE CASES LEARN GET INVOLVED



HOUSING



toolkit.unhabitat.org

OPEN SPACES



URBANIZATION



PUBLIC
TRANSPORT



<https://eotoolkit.unhabitat.org/>

SDG 11.3.1

Earth Engine Apps

1 Select city Lagos

admin level Province/County/State level

or draw an area of interest.

Rectangle Polygon Point

2 Select population data

GHS-Pop 1km of 2015

Vis_pop_min 300 Vis_pop_max 1500

Pop_density_TH 300 Pop_cluster_TH 1000000

[Download City Definition: Lagos2015-GHS-Pop 1km](#)

Secondary Indicators

Land Consumption per Capita: 200...

Indicator	Value
Built-up (km²)	~1000
Population (*10,000)	~0.027
LCPC (m²/person)	~0.593

Change in Urban Infill: 2000-2015...

Indicator	Value
Built-up T1 (km²)	~1000
Built-up T2 (km²)	~1000

Calculate SDG indicator 11.3.1

! Make sure you have generated the city definition!

1 Select data.

Built-up GHS-Built 38m

Population GHS-Pop 250m

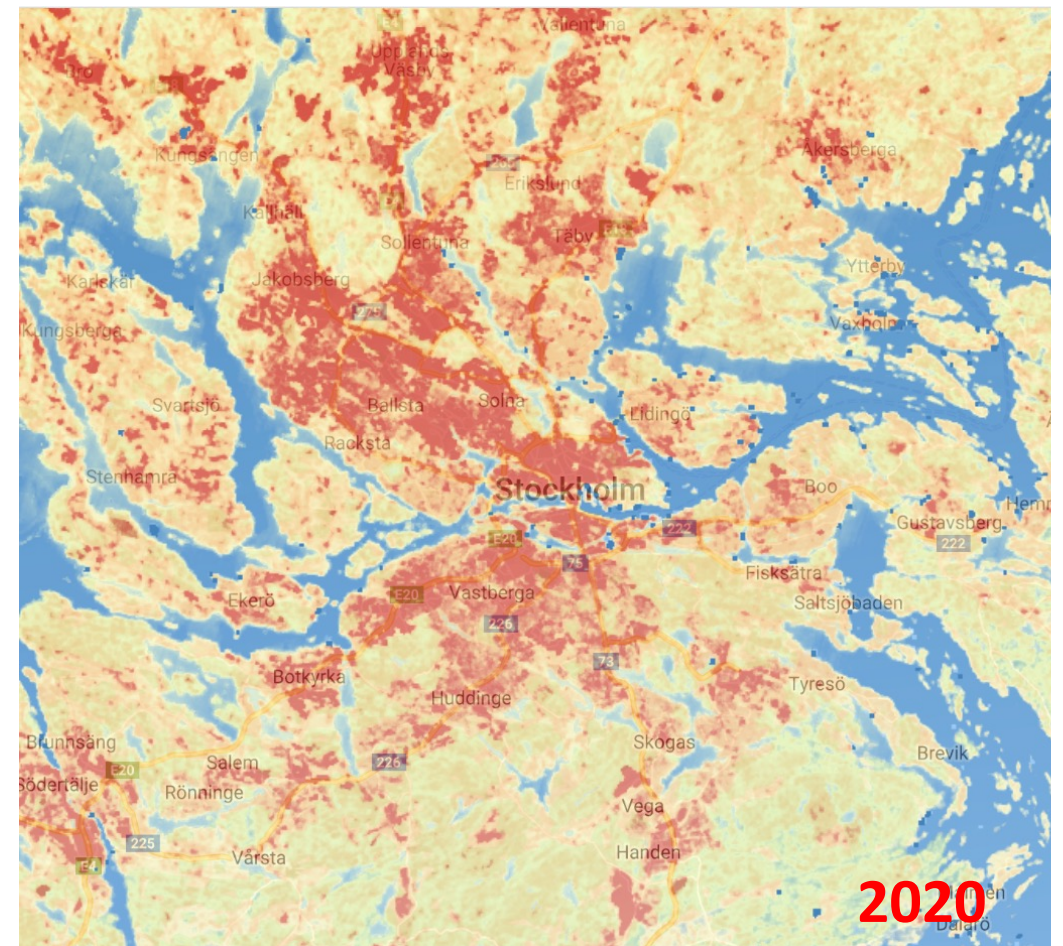
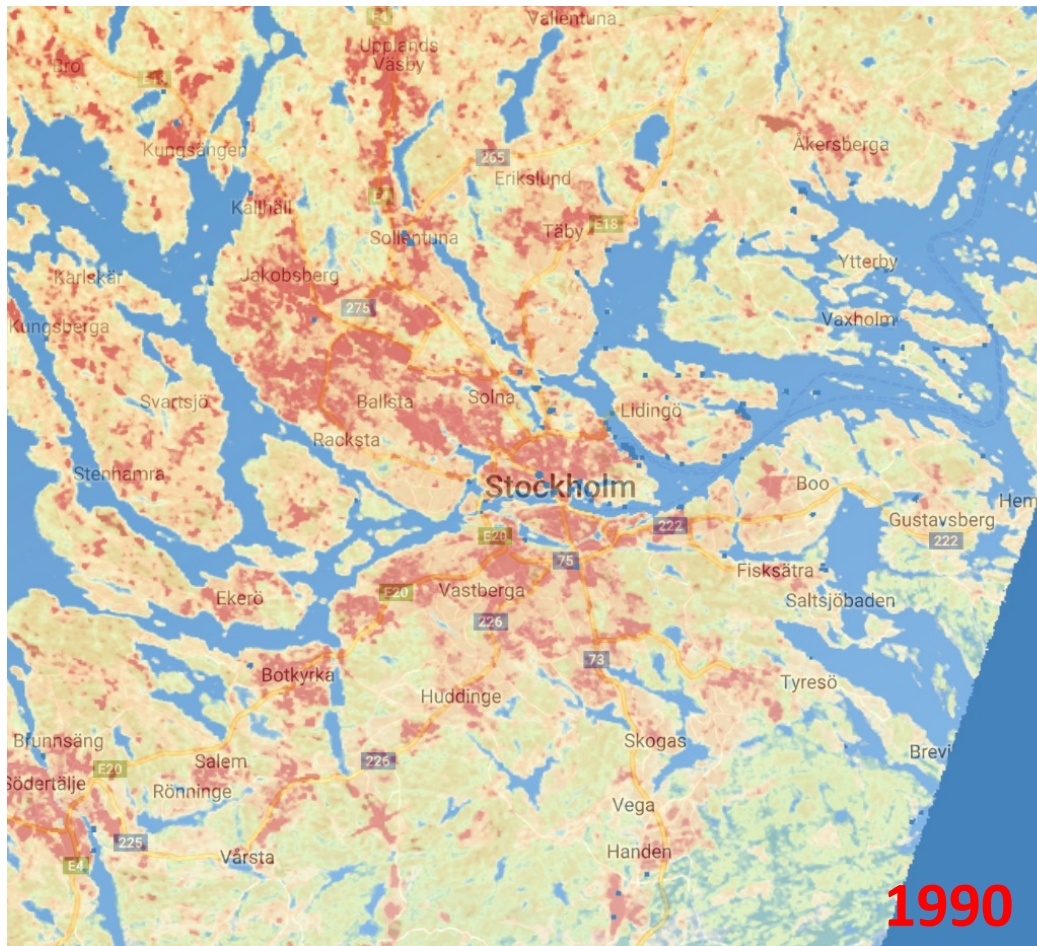
2 Select start year.

2000

[Download City Definition: Lagos2000-GHS-Pop 1km](#)

<https://eo4sdg11.users.earthengine.app/view/city-definition>
<https://eo4sdg11.users.earthengine.app/view/sdg11.3.1>

Land Surface Temperature: 1990 vs. 2020





学术报告



报告题目: EO-AI4GlobalChange: Earth Observation
Big Data and Deep Learning for Global
Environmental Change Monitoring

报告人: 班艺舫

瑞典皇家理工大学 首席教授、主任
瑞典数字未来中心 副主任
ICA 传感器驱动制图委员会 联合主席
IEEE TGRS 副主编



报告人简介:

班艺舫教授, 南京大学地理学学士、硕士, 加拿大滑铁卢大学博士。聚焦可持续和韧性发展, 班艺舫教授在地球观测大数据分析、机器学习/深度学习及其在环境变化监测应用(例如城市化、林火、洪水)等方面开展了大量研究, 负责EO4SmartCities、EO-AI4Urban、EO-AI4GlobalChange等重要国际科研项目, 取得了国际一流的学术成就。班艺舫教授还担任了联合国人居署可持续发展目标(SDG)人类住区指标技术委员会的特邀专家、GEO“全球城市观测和信息”的联合负责人以及国际主要遥感会议委员会的委员。

主持人: 杜培军 教授

时间: 2023年5月5日(星期五) 10:00-12:00

地点: 昆山楼B537会议室

欢迎各位老师同学参加!

南京大学地理与海洋科学学院
自然资源部国土卫星遥感应用重点实验室
江苏省地理信息技术重点实验室
江苏省遥感与地理信息系统学会



Name	Institution	Poster title	Contribution including period of research
Sebastian Hafner	KTH Royal Institute of Technology	Multi-Modal Deep Learning for Multi-Temporal Urban Mapping with a Partly Missing Modality	2020 – Present; Urban Mapping and Change Detection with Sentinel-1/-2 Time Series and Deep Learning

Name	Institution	Poster title	Contribution including period of research
Yuxi Sun	Harbin Institute of Technology Shenzhen	Multisource data reconstruction-based Deep Learning Unsupervised Hashing for Unisource Remote Sensing Image Retrieval	2021- Present; Deep Learning, Remote Sensing Image Retrieval